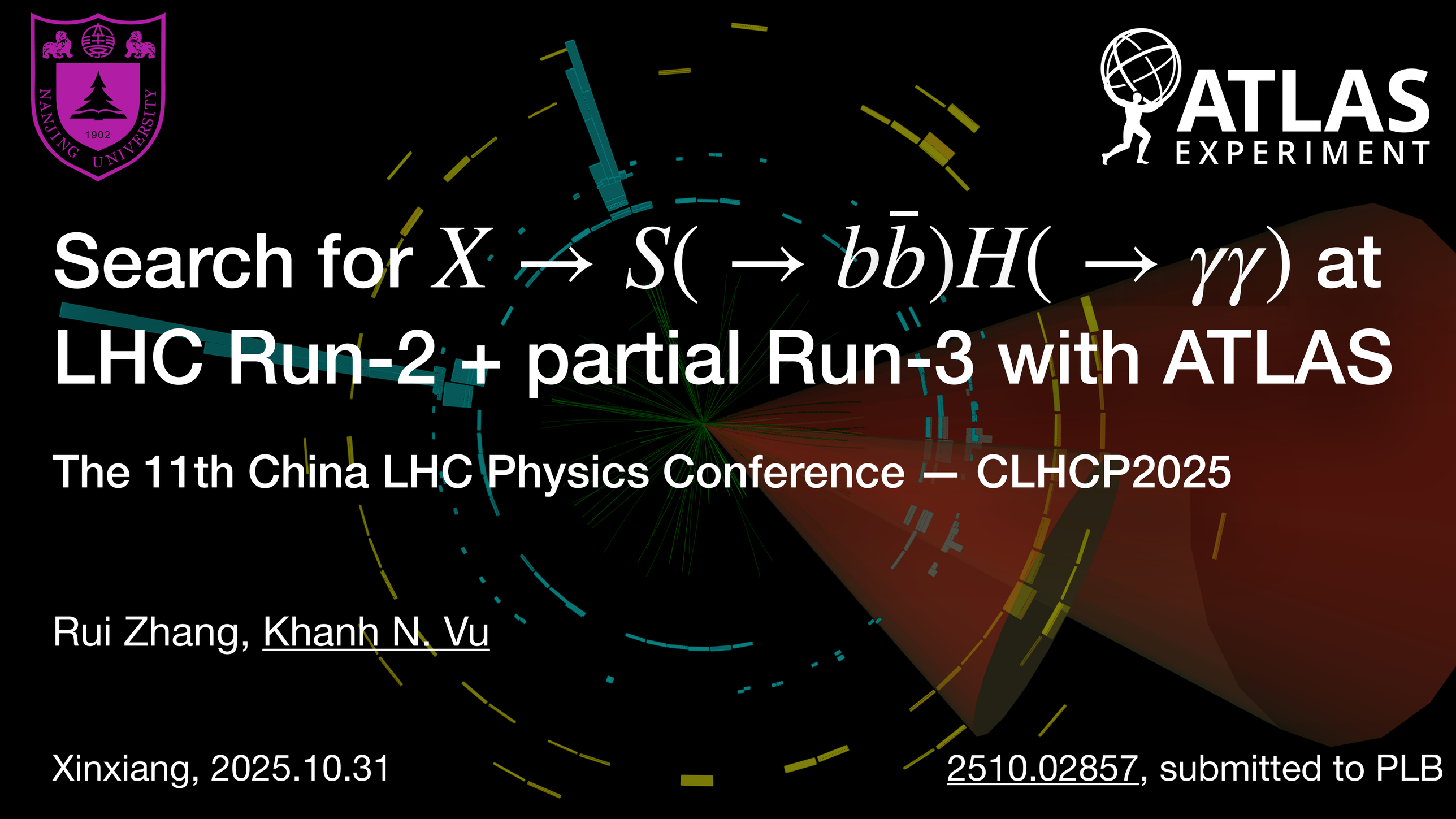

Search for $X \to S(\to b\bar{b})H(\to \gamma\gamma)$ at LHC Run-2 + partial Run-3 with ATLAS

The 11th China LHC Physics Conference — CLHCP2025

Rui Zhang, Khanh N. Vu

Xinxiang, 2025.10.31

2510.02857, submitted to PLB

Introduction

- $X \to SH$: ***distinctive experimental signatures*** characteristic of ***BSM models with an extended scalar sector*** e.g 2HDM, 2HDM+S, NMSSM.

- Published Run-2 searches for $X \to S(\to b\bar{b})H(\to \gamma\gamma)$

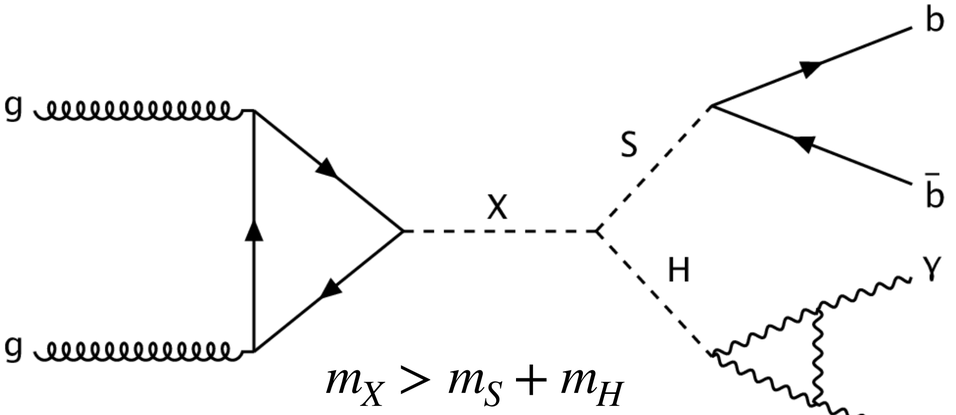

$m_X > m_S + m_H$

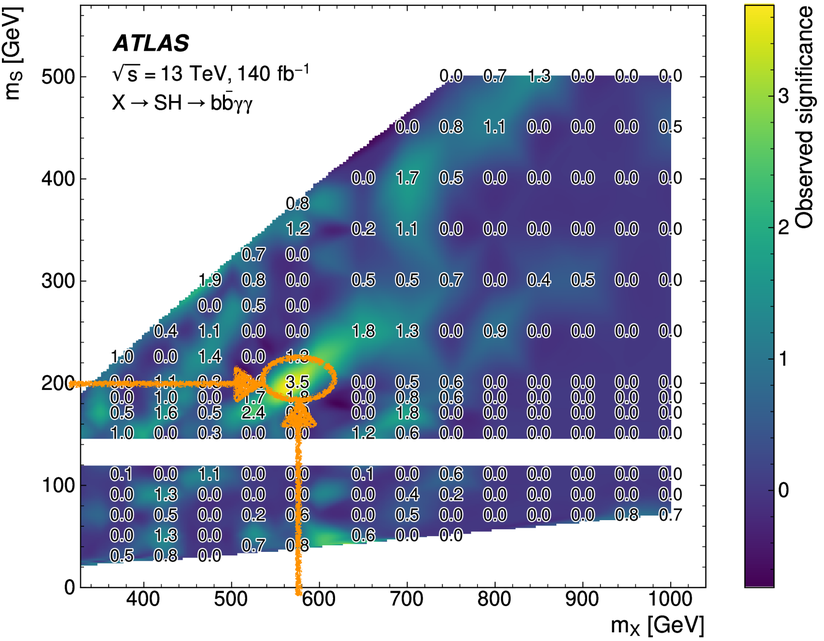

ATLAS [JHEP 11 (2024) 047)]

excess at $(m_X, m_S) = (575,200)$ GeV GeV with a *local (global) significance of* $3.5\ (2.0)\ \sigma$

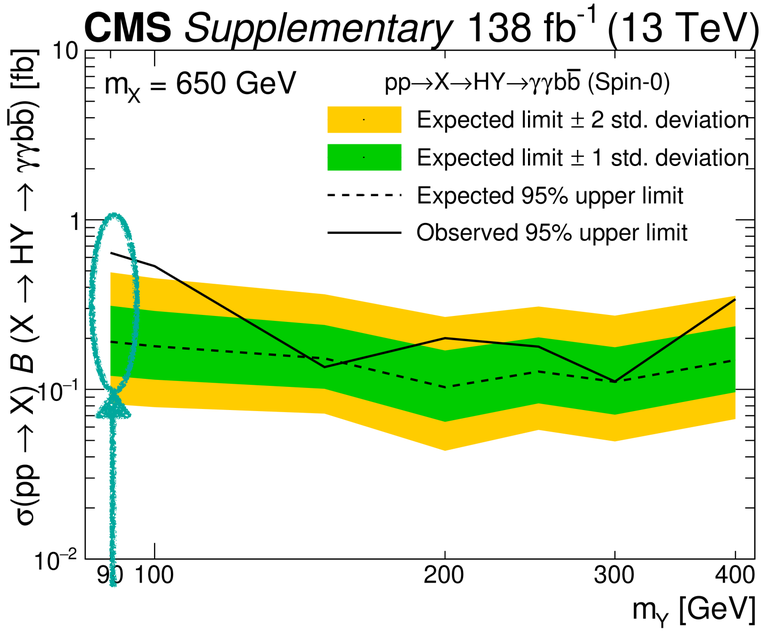

CMS [JHEP 05 (2024) 316]

excess at $(m_X, m_S) = (650,90)$ GeV GeV with a *local (global) significance of* $3.8\ (2.8)\ \sigma$

Introduction

- $X \to SH$: ***distinctive experimental signatures*** characteristic of ***BSM models with an extended scalar sector*** e.g 2HDM, 2HDM+S, NMSSM.

- Published Run-2 searches for $X \to S(\to b\bar{b})H(\to \gamma\gamma)$

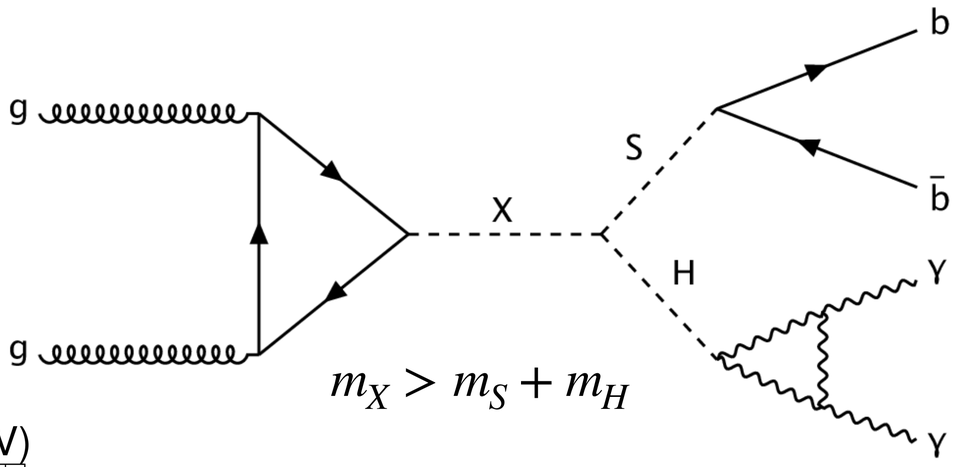

$m_X > m_S + m_H$

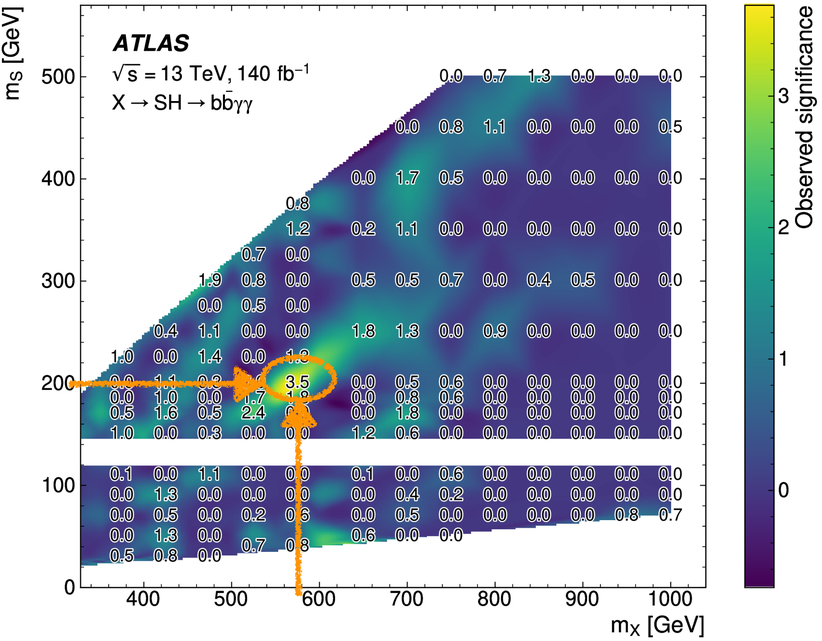

ATLAS [JHEP 11 (2024) 047)]

excess at $(m_X, m_S) = (575,200)$ GeV GeV with a *local (global) significance of* $3.5\ (2.0)\ \sigma$

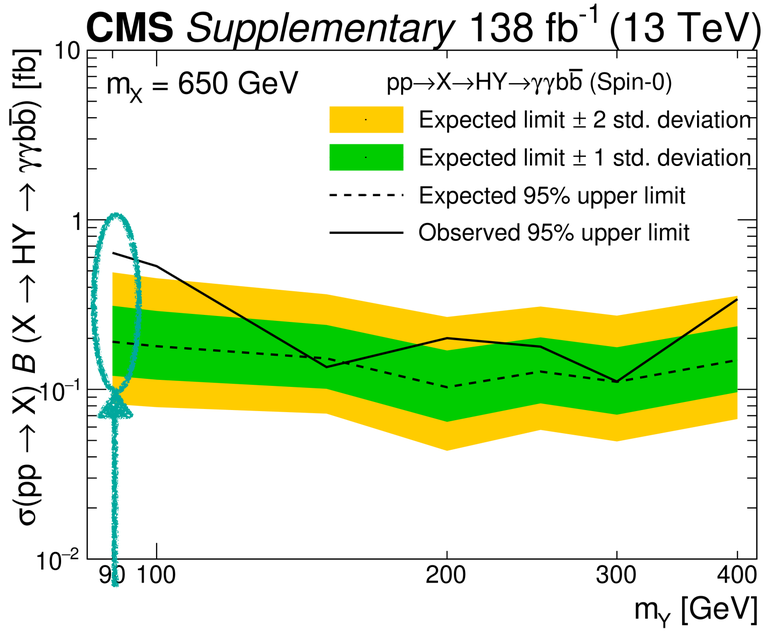

CMS [JHEP 05 (2024) 316]

excess at $(m_X, m_S) = (650,90)$ GeV GeV with a *local (global) significance of* $3.8\ (2.8)\ \sigma$

Goal of this study

- *Fast and timely follow-up* with an updated search *to re-examine excesses observed in Run-2*, using
  - ***Full Run-2 + partial Run-3*** data;
  - overall similar strategy with ***improvements*** in ***object reconstruction/identification***, ***training of disc. variable***, and ***signal region definition***.
- *Set things up for the next iteration with full Run-3 dataset used*.

Data and MC samples

Data:

- Run-2: 2015 - 2018 @ $\sqrt{s} = 13$ TeV; 140 fb^{-1}.
- *Run-3: 2022 - 2023 @ $\sqrt{s} = 13.6$ TeV; 58.6 fb^{-1}.*
- *selected using ONLY diphoton triggers*.

MC signal samples:

- generated at LO in ggF mode, with Narrow-Width Approximation of $\Gamma_X = \Gamma_S = 10$ MeV; *AF3 for detector response*.
- 160 (m_X, m_S) mass points

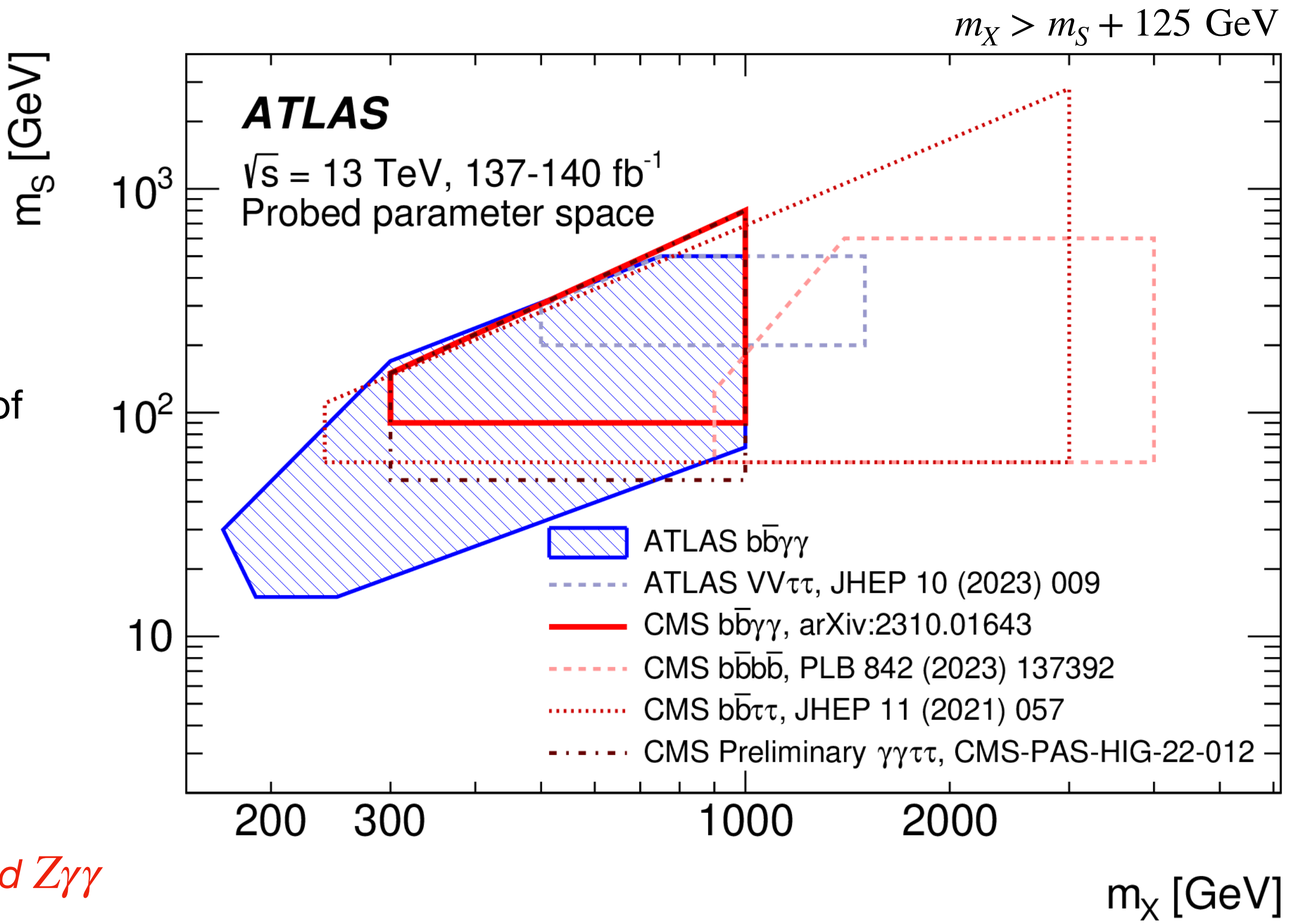

MC background samples:

- Continuum non-resonant diphoton: $\gamma\gamma + \text{jets}$, *$t\bar{t}\gamma\gamma$, and $Z\gamma\gamma$:*
  - *Newer Sherpa samples and processed with AF3 for $\gamma\gamma + \text{jets}$ and $Z\gamma\gamma$*
- Single- and Di-Higgs processes with $H \to \gamma\gamma$:
  - generated with Powheg or Madgraph, considering VBF H/HH, ggF H/HH, VH, $t\bar{t}H$, etc.

**in red highlighting changes wrt ATLAS Run-2 only iteration*

Data and MC samples

Data:

- Run-2: 2015 - 2018 @ $\sqrt{s} = 13$ TeV; 140 fb^{-1}.
- *Run-3: 2022 - 2023 @ $\sqrt{s} = 13.6$ TeV; 58.6 fb^{-1}.*
- *selected using ONLY diphoton triggers*.

MC signal samples:

- generated at LO in ggF mode, with Narrow-Width Approximation of $\Gamma_X = \Gamma_S = 10$ MeV; *AF3 for detector response*.
- 160 (m_X, m_S) mass points *probing* $170 \leq m_X \leq 1000$ GeV, $15 \leq m_S \leq 500$ GeV$\rightarrow$ *unique sensitivity in low-mass region*

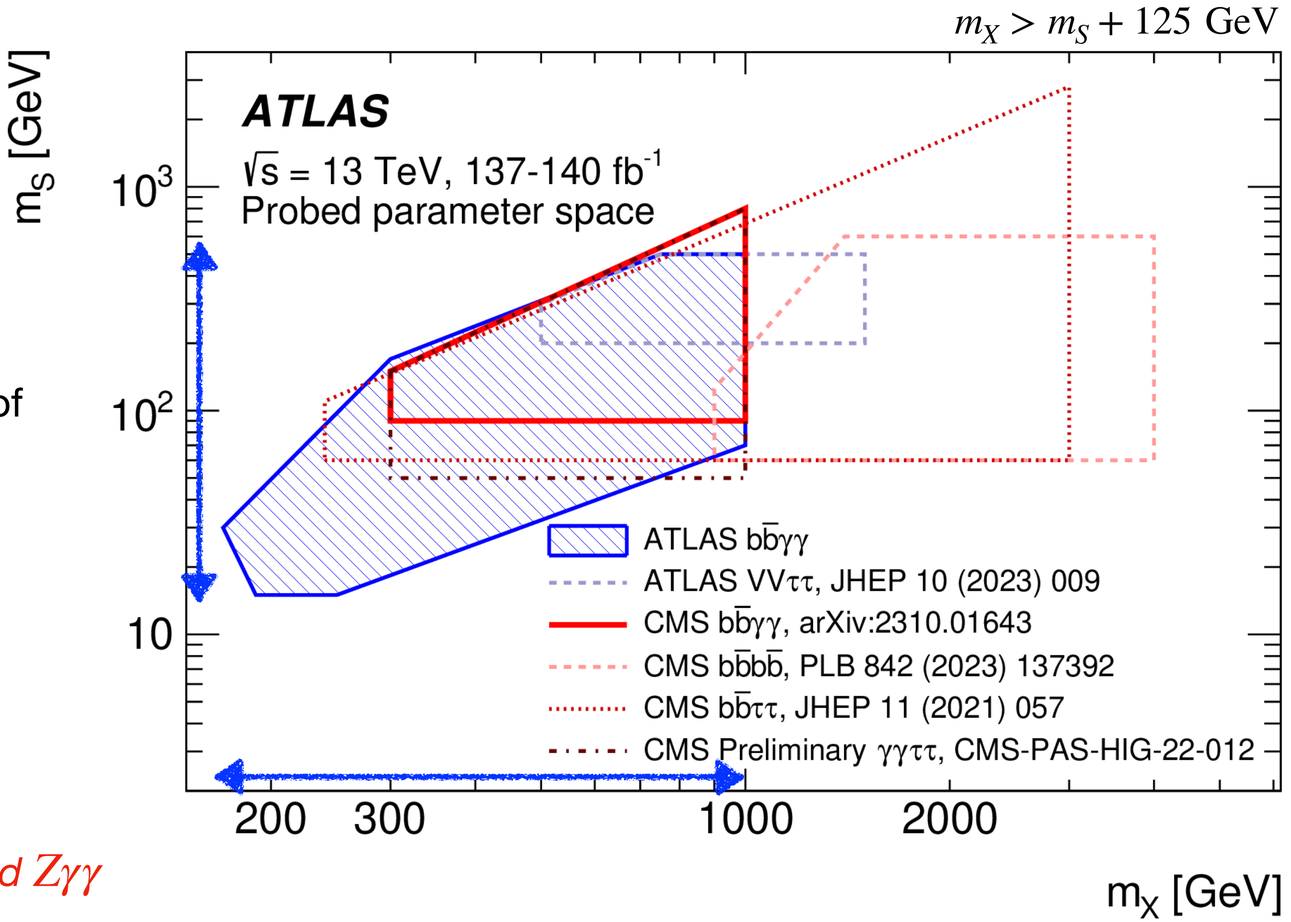

MC background samples:

- Continuum non-resonant diphoton: $\gamma\gamma + \text{jets}$, *$t\bar{t}\gamma\gamma$, and $Z\gamma\gamma$:*
  - *Newer Sherpa samples and processed with AF3 for $\gamma\gamma + \text{jets}$ and $Z\gamma\gamma$*
- Single- and Di-Higgs processes with $H \rightarrow \gamma\gamma$:
  - generated with Powheg or Madgraph, considering VBF H/HH, ggF H/HH, VH, $t\bar{t}H$, etc.

**in red highlighting changes wrt ATLAS Run-2 only iteration*

Object definitions

Vertex

- *using standard ATLAS definition: highest Σp_{T}^2 from all associated tracks with $p_{\mathrm{T}} > 500$ MeV.*

Photons

- **ID**: *Tight WP* with $|\eta| < 2.37$, excluding $1.37 < |\eta| < 1.52$
- **Isolation**: *FixedCutLoose WP* with $|\mathrm{topoEtCone20}| < 0.065 \times p_{\mathrm{T}}^{\gamma}$ and $|\mathrm{ptcone20}/p_{\mathrm{T}}^{\gamma}| < 0.05 \times p_{\mathrm{T}}^{\gamma}$

Jets

- PFlow $R = 0.4$ anti-k_t + JVT
- $p_{\mathrm{T}} > 25$ GeV; $|\eta| < 4.4$
- ***b*-tagging**: *updated to GN2 @ 85%, offering substantial improvements (by 8% in tagging efficiency) over DL1r @ 77% (used in previous round)*. Only applied for ***central jets*** ($|\eta| < 2.5$).

Leptons

- **Electrons**: $p_{\mathrm{T}} > 10$ GeV, $|\eta| < 2.47$; *MediumLH WP* for ID, while *Loose_VarRad WP* for isolation.
- **Muons**: $p_{\mathrm{T}} > 10$ GeV, $|\eta| < 2.7$; *Medium WP* for ID, while *PflowLoose_VarRad WP* for isolation.
- Matched to the primary vertex with $|z_0| \sin\theta < 0.5$ mm for e and μ, and $|d_0|/\sigma_{d_0} < 5$ (3) for e (μ).

Overlap removal

- Firstly, removing jets, electrons, muons within $\Delta R < 0.4$ of photons.
- Next, removing jets within $\Delta R < 0.2$ of electrons.
- Finally, removing electrons and muons within $\Delta R < 0.4$ of any remaining jets.

**in red highlighting changes wrt ATLAS Run-2 only iteration*

Event selection

	Preselection
N_γ	≥ 2
$m_{\gamma\gamma}$ [GeV]	∈ [105, 160]
$p_T(\gamma)/m_{\gamma\gamma}$	> 0.35 (0.25) for leading (subleading) photon
N_ℓ	= 0
$N_{central\text{-}jets}$	∈ [2, 5]
$N_{b\text{-}jets}$	= 1 or 2

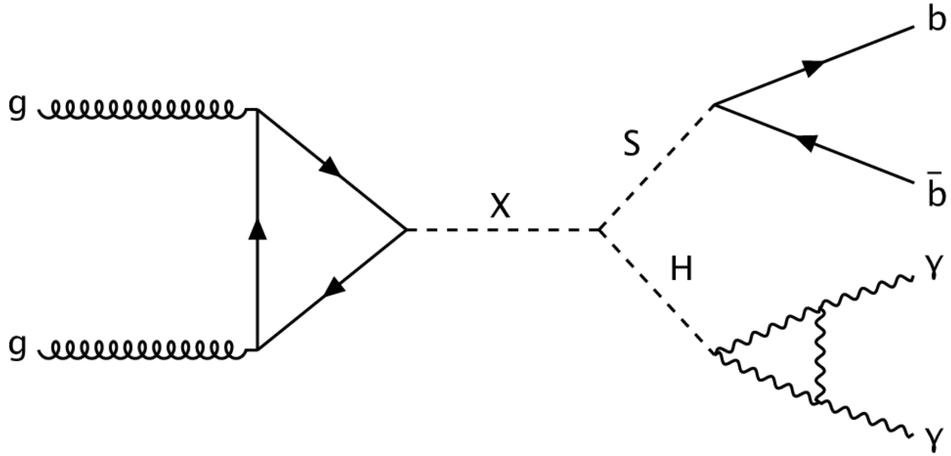

**in red highlighting changes wrt ATLAS Run-2 only iteration*

Event selection

	Preselection
N_γ	≥ 2
$m_{\gamma\gamma}$ [GeV]	∈ [105, 160]
$p_T(\gamma)/m_{\gamma\gamma}$	> 0.35 (0.25) for leading (subleading) photon
N_ℓ	= 0
$N_{central\text{-}jets}$	∈ [2, 5]
$N_{b\text{-}jets}$	= 1 or 2

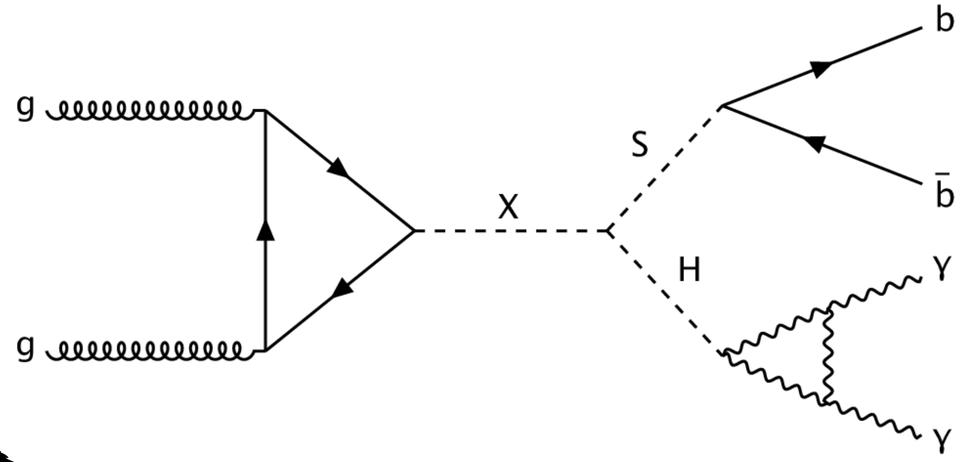

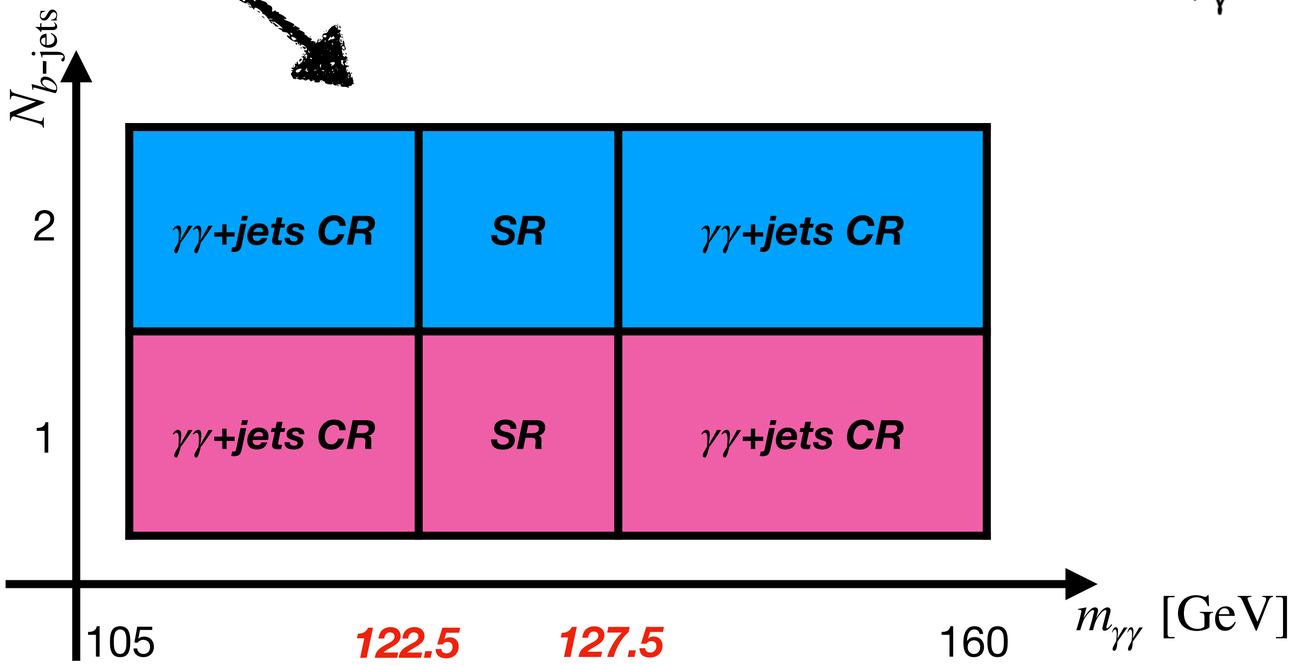

Narrower $m_{\gamma\gamma}$ window compared to previous analysis, reducing 1/2 background contamination in SR

*in red highlighting changes wrt ATLAS Run-2 only iteration

Event selection

	Preselection
N_γ	≥ 2
$m_{\gamma\gamma}$ [GeV]	∈ [105, 160]
$p_T(\gamma)/m_{\gamma\gamma}$	> 0.35 (0.25) for leading (subleading) photon
N_ℓ	= 0
$N_{central\text{-}jets}$	∈ [2, 5]
$N_{b\text{-}jets}$	= 1 or 2

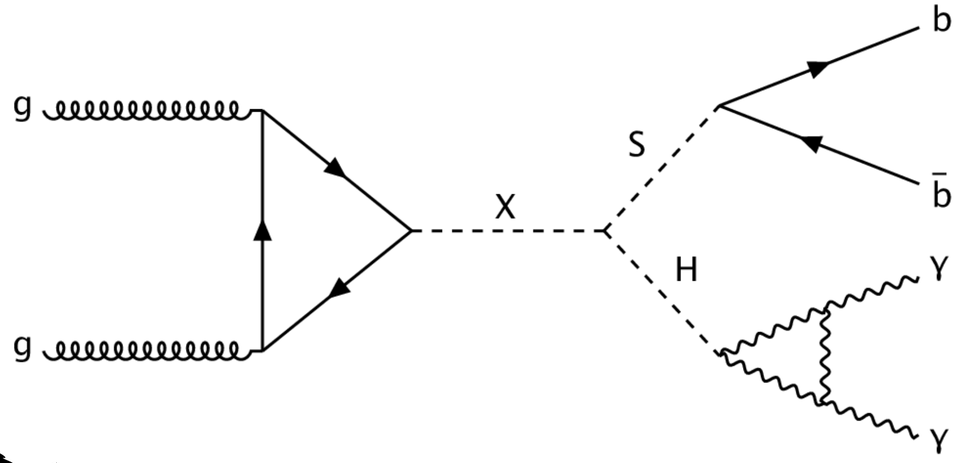

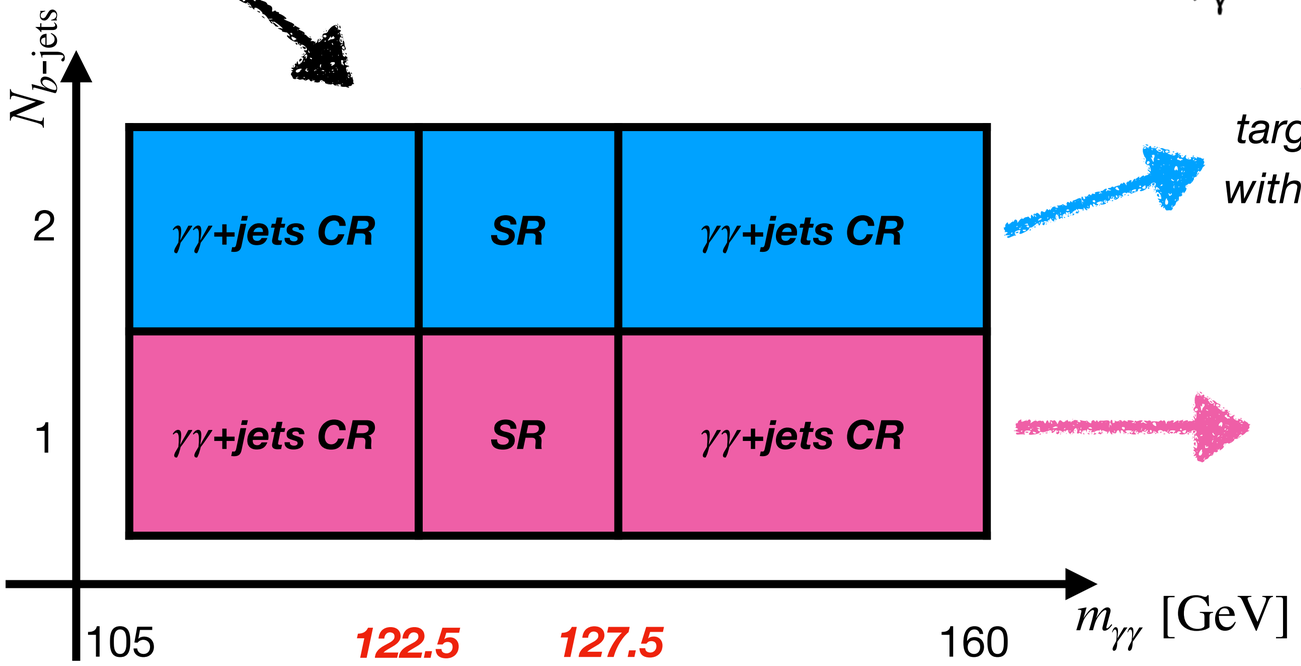

2 b-tagged
targets 132 signals with $m_S/m_X \geq 0.09$

1 b-tagged
targets 28 signals with $m_S/m_X < 0.09$

Narrower $m_{\gamma\gamma}$ window compared to previous analysis, reducing 1/2 background contamination in SR

**in red highlighting changes wrt ATLAS Run-2 only iteration*

Multivariate analysis

$$m^*_{b\gamma\gamma} = m_{b\gamma\gamma} - (m_{\gamma\gamma} - 125\ \text{GeV})$$
$$m^*_{bb\gamma\gamma} = m_{bb\gamma\gamma} - (m_{\gamma\gamma} - 125\ \text{GeV})$$

- ***Parameterised Neural Networks (PNNs)***
  - used to separate signal from background in SR.
  - provide sensitivity over considered mass range and *allow interpolation to $(m_X,\ m_S)$ not included in training*.

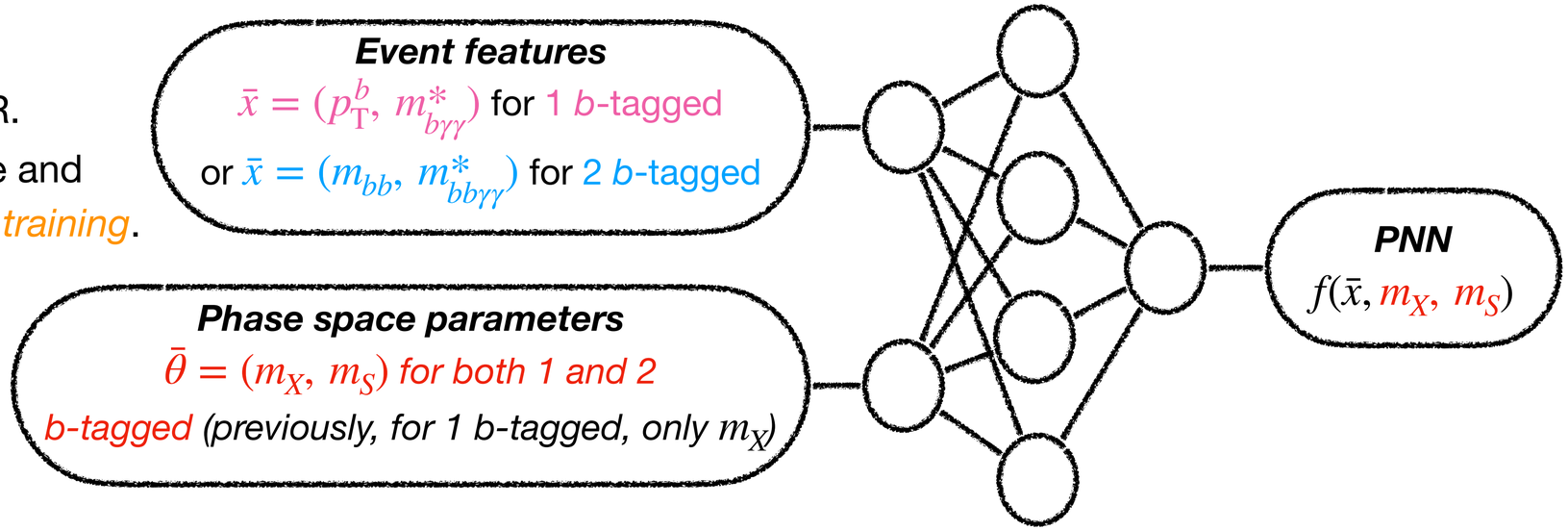

*in red highlighting changes wrt ATLAS Run-2 only iteration

Multivariate analysis

$$m^*_{b\gamma\gamma} = m_{b\gamma\gamma} - (m_{\gamma\gamma} - 125\ \text{GeV})$$
$$m^*_{bb\gamma\gamma} = m_{bb\gamma\gamma} - (m_{\gamma\gamma} - 125\ \text{GeV})$$

- ***Parameterised Neural Networks (PNNs)***
  - used to separate signal from background in SR.
  - provide sensitivity over considered mass range and *allow interpolation to (m_X, m_S) not included in training*.

- ***4 separate PNNs** trained using all related signal and major background samples for **each of***

  [1 b-tagged, 2 b-tagged] × [Run-2, Run-3]

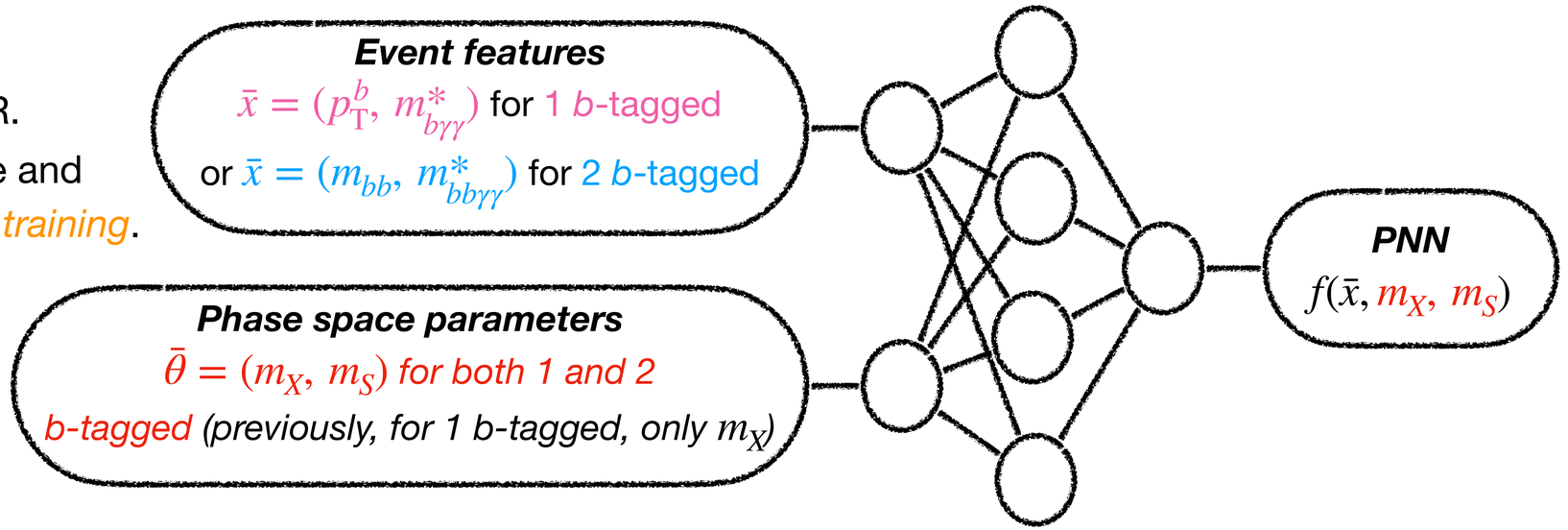

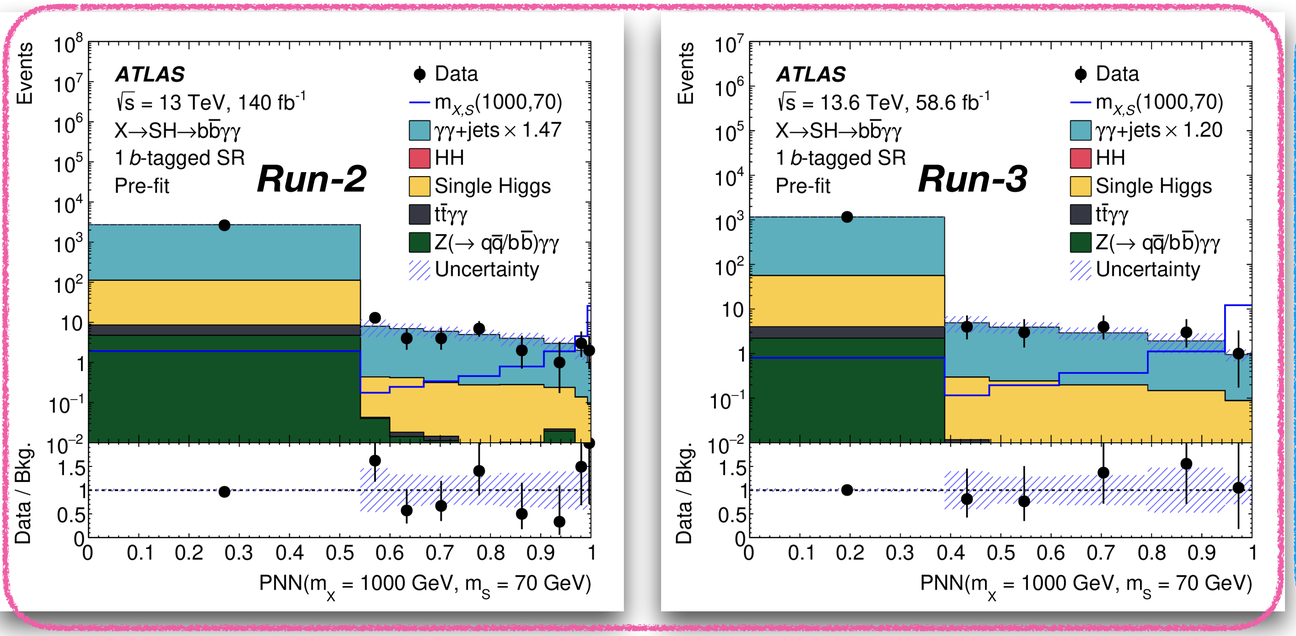

1 *b*-tagged

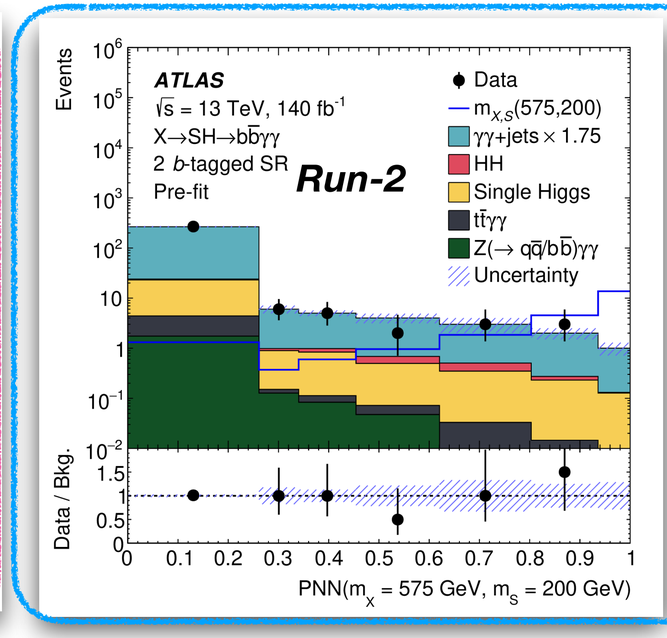

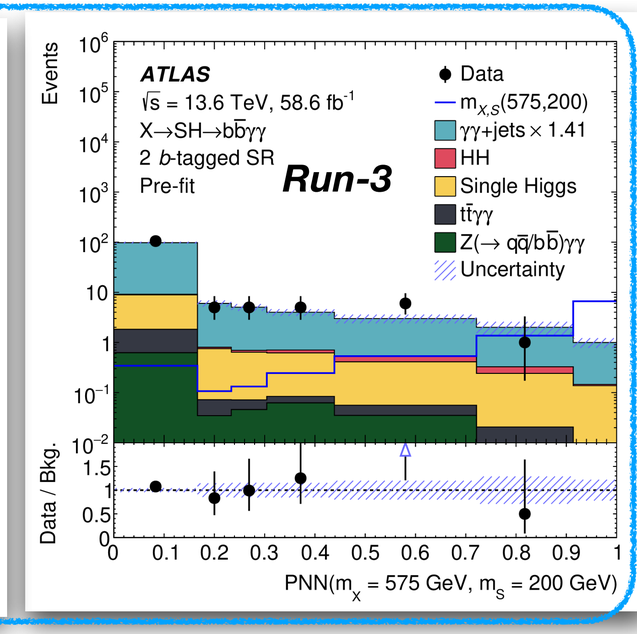

2 *b*-tagged

**in red highlighting changes wrt ATLAS Run-2 only iteration*

Background estimation

- H/HH, $t\bar{t}\gamma\gamma$, and $Z\gamma\gamma$ estimated directly from MC.

- $\gamma\gamma$ + jets ***estimation***:
  - ***norm factors*** from matching background prediction to data in CRs used to correct pre-fit shape in CRs and SRs, and then free-floating in the fit.

	Run-2	***Run-3***
1 b-tagged	1.47±0.02	1.20±0.03
2 b-tagged	1.75±0.04	1.41±0.05

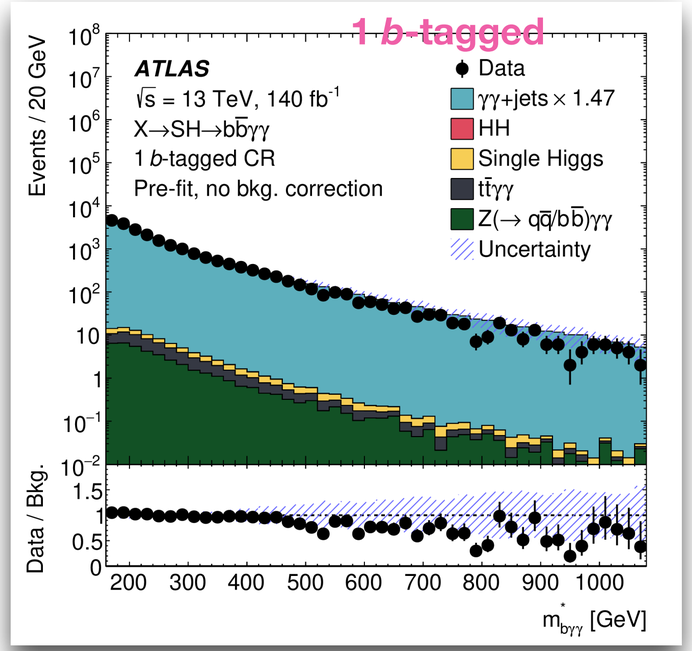

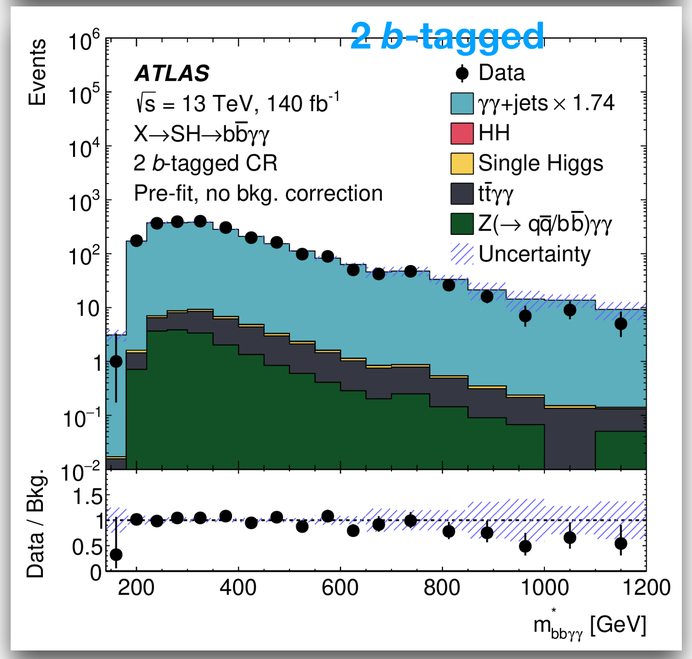

Background estimation

- H/HH, $t\bar{t}\gamma\gamma$, and $Z\gamma\gamma$ estimated directly from MC.

- $\gamma\gamma$ + jets ***estimation***:
  - ***norm factors*** from matching background prediction to data in CRs used to correct pre-fit shape in CRs and SRs, and then free-floating in the fit.

	Run-2	***Run-3***
1 b-tagged	1.47±0.02	1.20±0.03
2 b-tagged	1.75±0.04	1.41±0.05

  - Additional ***event-by-event correction*** based on ***linear fit*** of data/MC vs. $m^*_{b\gamma\gamma}$ ($m^*_{bb\gamma\gamma}$) in 1 (2) *b*-tagged CR applied to mitigate mismodelling of PNN distributions.

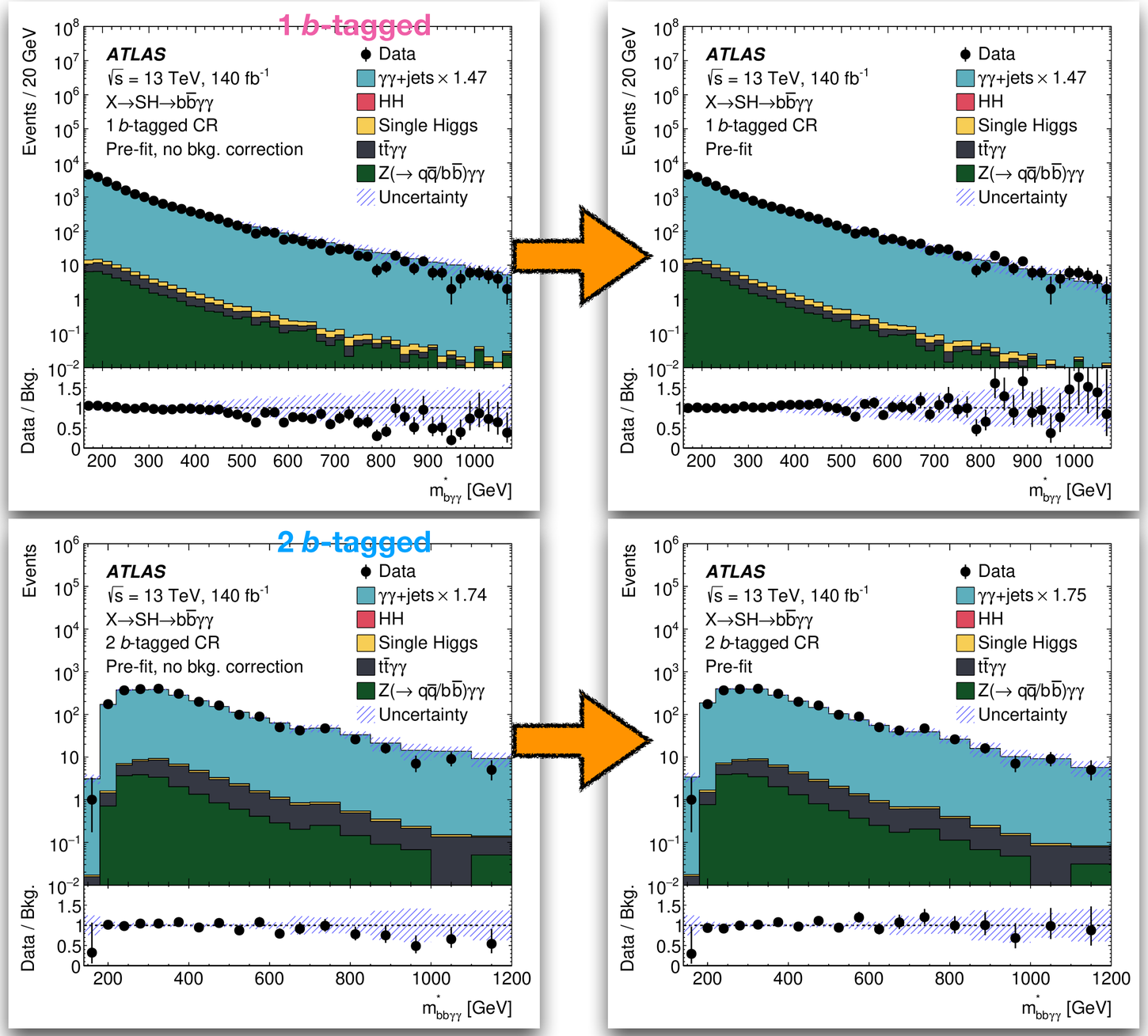

Signal interpolation

- ***200 additional mass points*** *interpolated in* $m_X \geq 300$ GeV *and* $m_S \geq 70$ GeV *for 2 b-tagged category* to be sensitive to whole parameter space.

- ***Interpolation method***:
  - ***Rescaling***: kinematics of interpolated mass points emulated from a high-statistics reference sample by rescaling reconstructed four-vectors of H and S in X's rest-frame so that they are distributed around theoretical values of the interpolated point.
  - ***Reweighting***:
    - Ref. sample events weighted to reproduce interpolated point's m_{bb} resolution.
    - m_{bb} resolution of simulated points modelled with ***Bukin PDF***.
    - m_{bb} resolution of interpolated points extracted from interpolation of Bukin paramaters using ***Delaunay triangulation.***

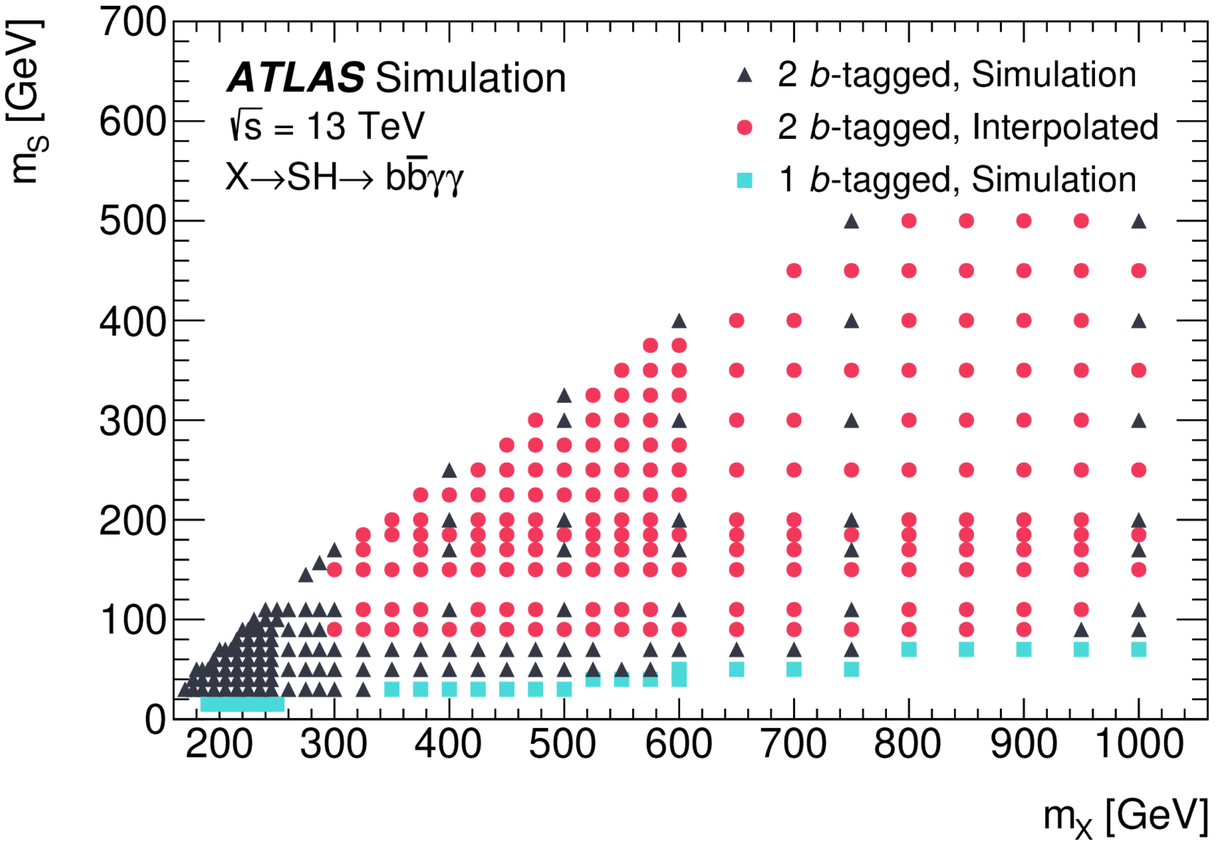

Systematic uncertainties

- ***Experimental uncertainties***: luminosity, diphoton trigger, photon and jet energy scale and resolution, photon identification, jet flavor tagging.

- ***Theoretical uncertainties***:
  - QCD scale, PDFs + α_s, Parton Showering modelling, and cross-section predictions.
  - normalisation of single-Higgs processes with heavy flavour at LO (100%)
  - $H \to \gamma\gamma$ and $H \to bb$ branching ratios.

- *$\gamma\gamma + \text{jets}$ related uncertainties:*
  - *modelling and normalisation extrapolation from CR to SR.*
  - *event-by-event linear correction of $\gamma\gamma + \text{jets}$ PNN.*

- ***Uncertainty for signals from interpolation**.*

- *Computed independently for Run-2 and Run-3 as well as for 1 b-tagged and 2 b-tagged categories*.

- *Uncertainties in lumi, $\gamma\gamma + \text{jets}$ NFs, flavour-tagging and all related to photon UNCORRELATED between Run-2 and Run-3, while the rest fully correlated*.

Statistical method

- *Likelihood function for a particular b-tagged category and for a given data-taking run*

$$\mathcal{L} = \underbrace{\text{Pois}\left(n_{\text{SB}} \middle| \mu_{\gamma\gamma} N_{\text{SB}}^{\gamma\gamma}(\boldsymbol{\theta}) + \sum_p N_{\text{SB}}^{p}(\boldsymbol{\theta})\right)}_{\text{Single-bin sideband CR}} \cdot \underbrace{\prod_i \text{Pois}\left(n_{\text{SR},i} \middle| \mu_{\gamma\gamma} N_{\text{SR}}^{\gamma\gamma}(\boldsymbol{\theta}) f_i^{\gamma\gamma}(\boldsymbol{\theta}) + \sum_p N_{\text{SR}}^{p}(\boldsymbol{\theta}) f_i^{p}(\boldsymbol{\theta})\right)}_{\text{Binned PNN output distribution in SR}} \cdot G(\boldsymbol{\theta})$$

- Maximum-likelihood fit performed ***separately for 1 and 2 b-tagged*** categories but ***simultaneously for Run-2 and 3***.
- Binning of PNN optimised independently for each signal and each data-taking run.
- upper limits on $\mu \equiv \dfrac{[\sigma_{13\ \text{TeV}}]_{\text{obs}}}{[\sigma_{13\ \text{TeV}}]_{\text{exp}}} \equiv \dfrac{[\sigma_{13.6\ \text{TeV}}]_{\text{obs}}}{[\sigma_{13.6\ \text{TeV}}]_{\text{exp}}}$ are derived using ***profile-likelihood-ratio test statistic*** and ***CLs method***
- Then deriving upper limits on $\sigma_{13\ \text{TeV}}$ assuming $[\sigma_{13\ \text{TeV}}]_{\text{exp}}$ equal to observed limits from previous Run-2 only analysis.

Local significances

ATLAS Run-2 only analysis

[JHEP 11 (2024) 047)]

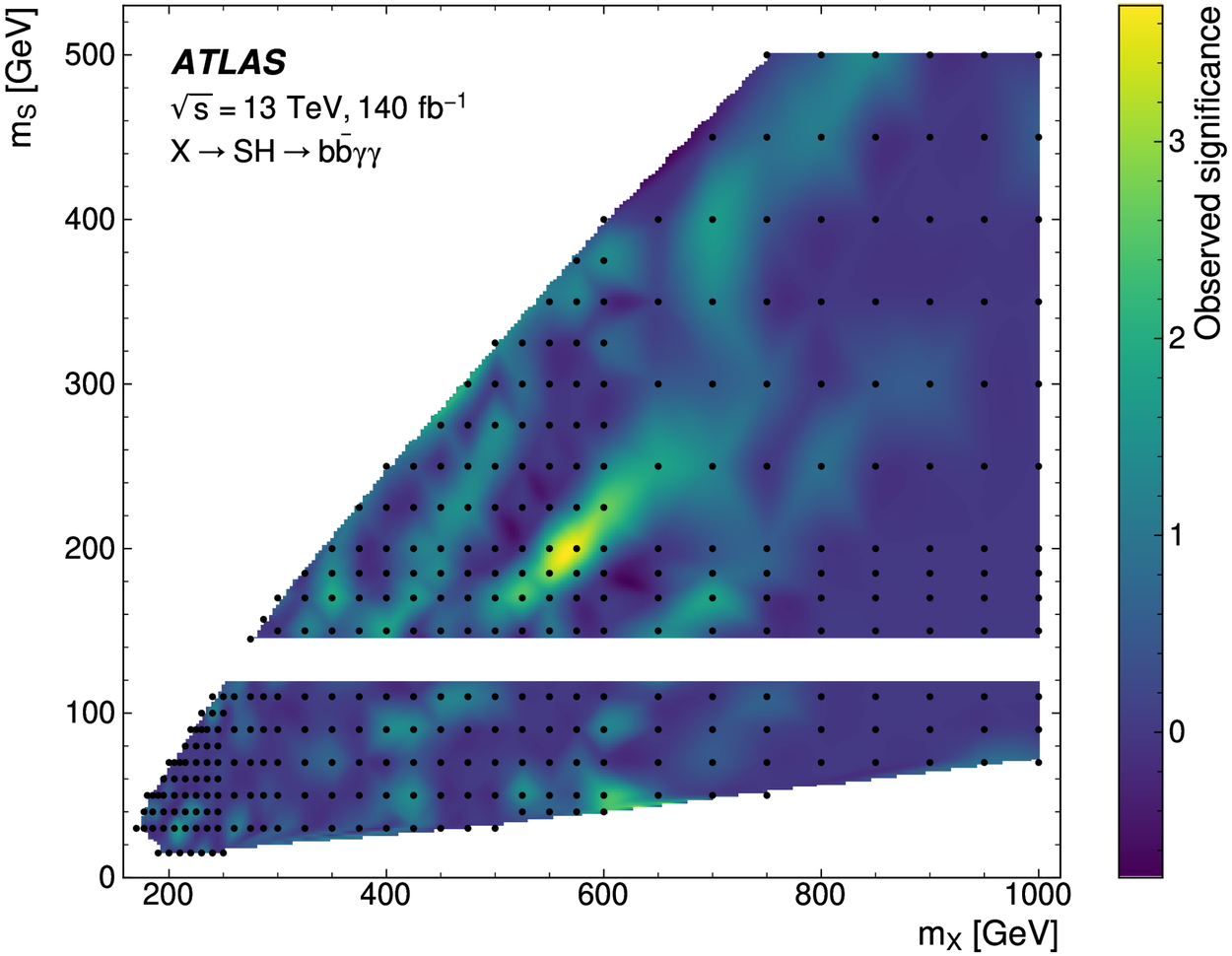

Our analysis using Run-2 + partial Run-3 data

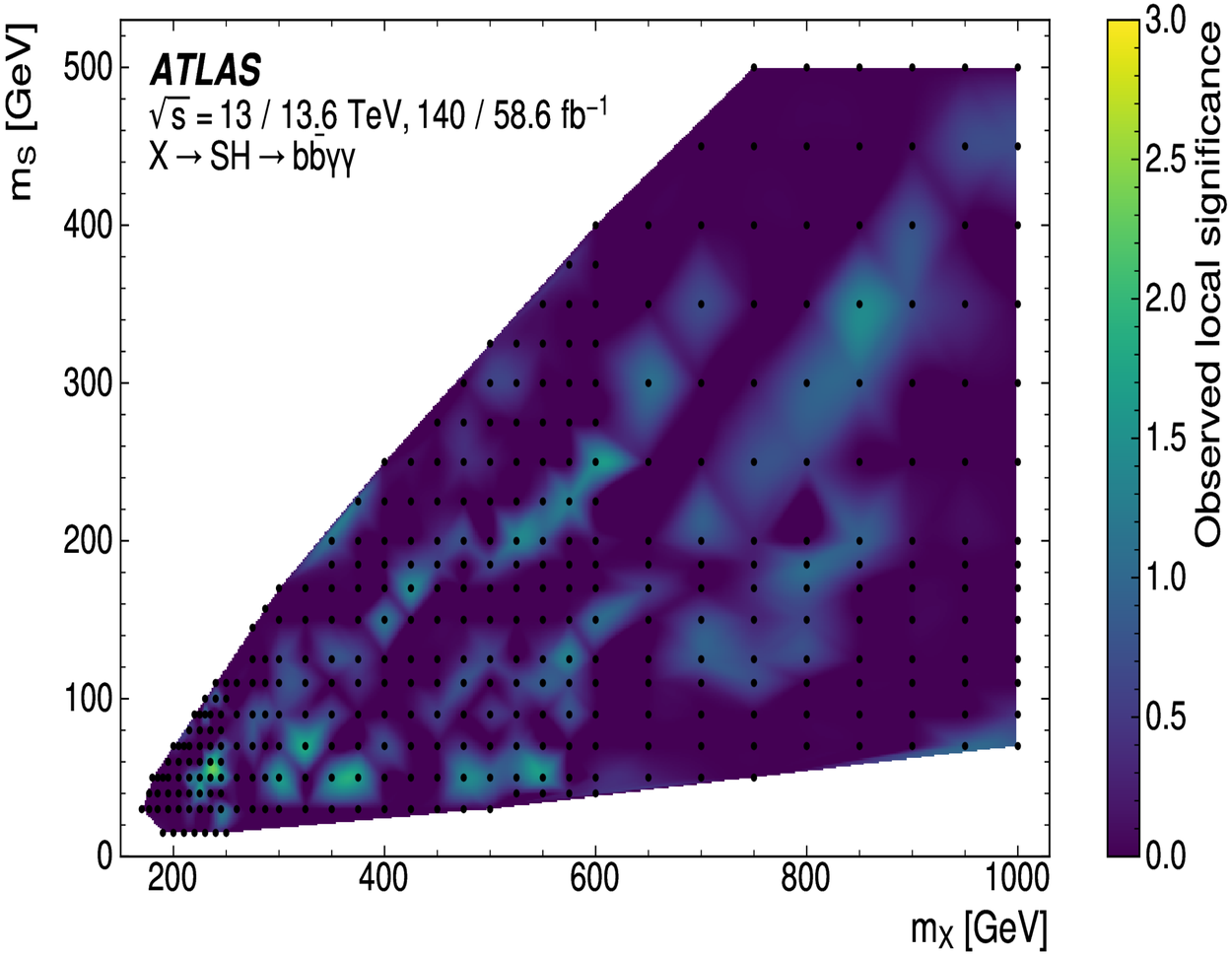

Local significances

ATLAS Run-2 only analysis

[JHEP 11 (2024) 047)]

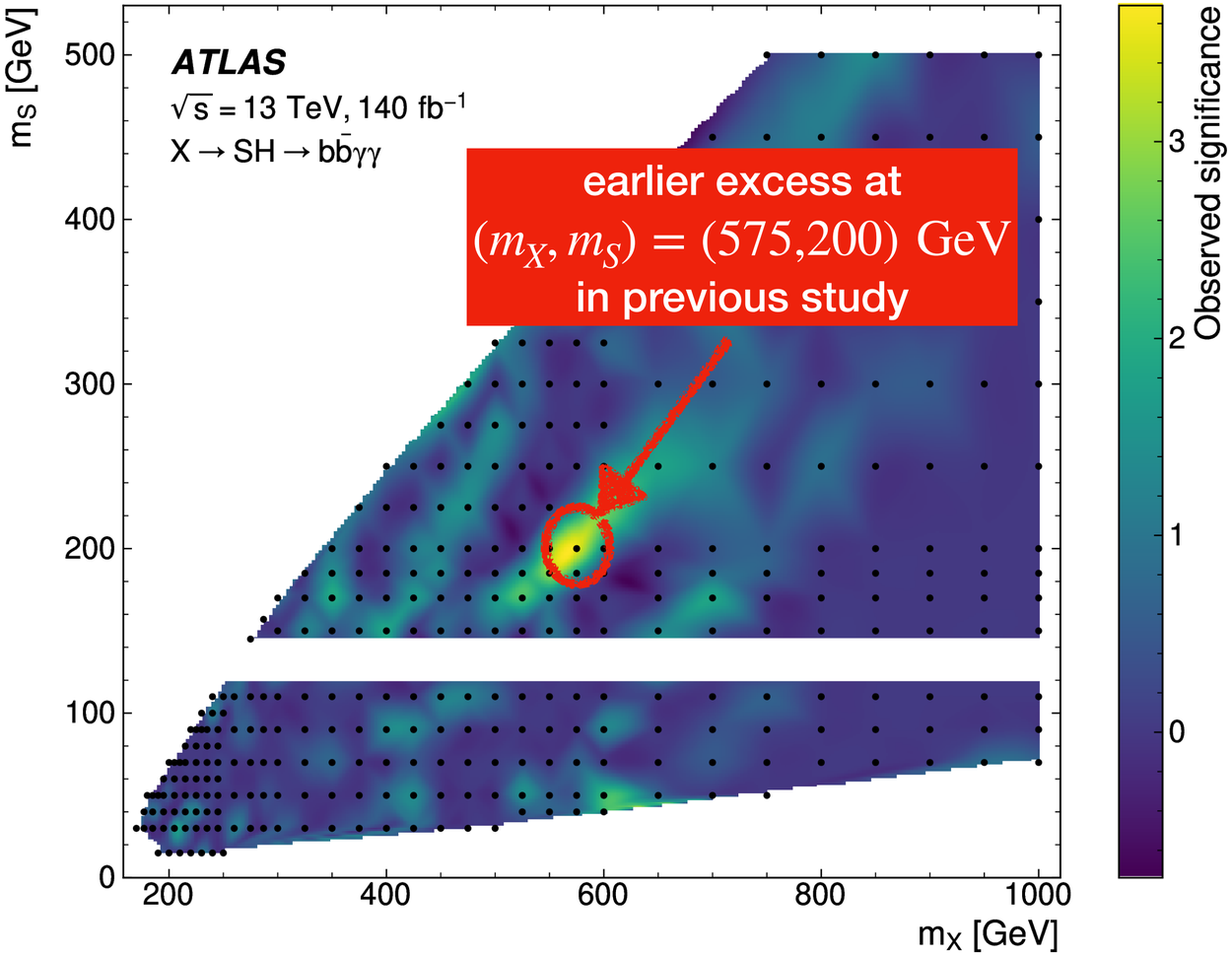

Our analysis using Run-2 + partial Run-3 data

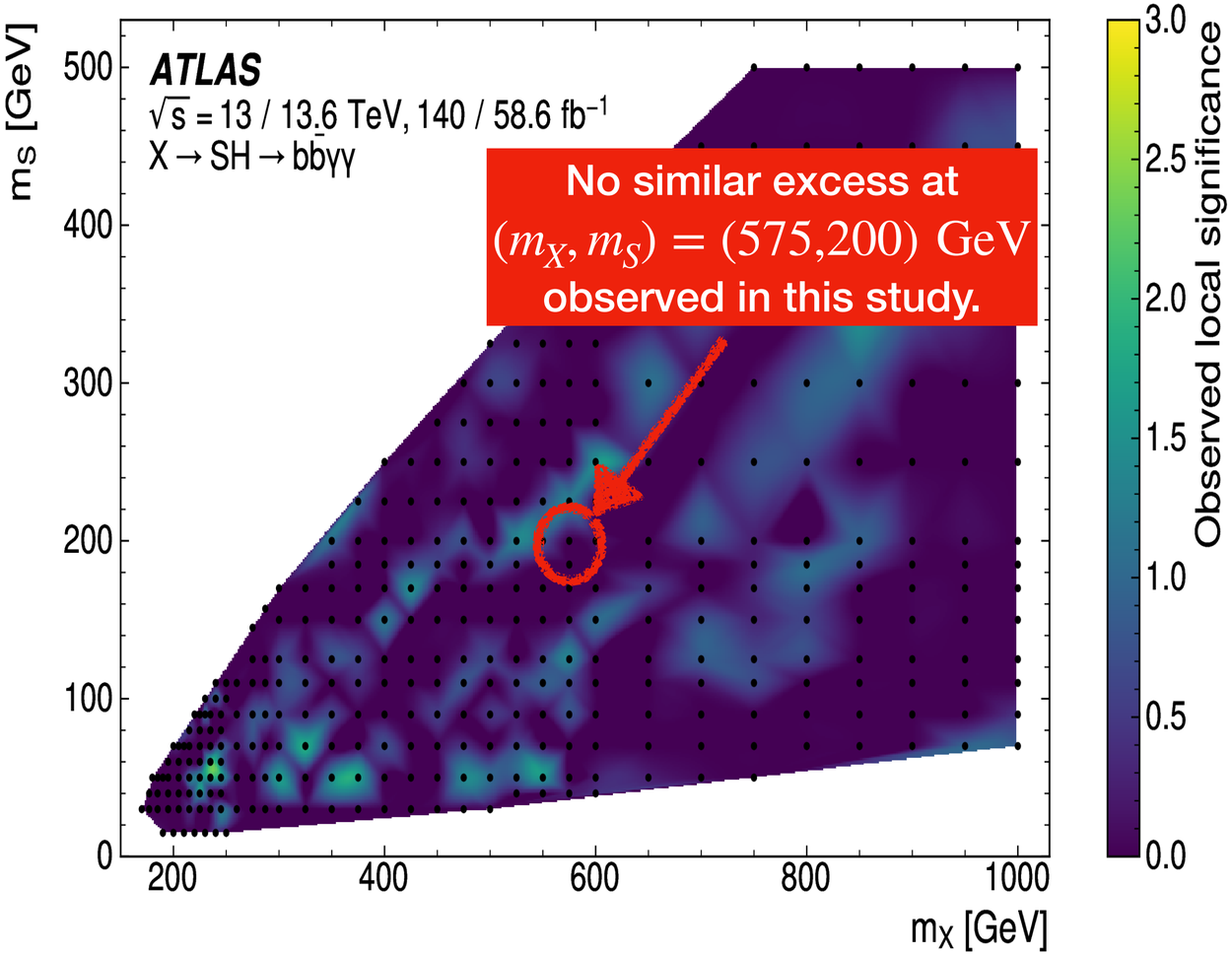

Local significances

ATLAS Run-2 only analysis

[JHEP 11 (2024) 047)]

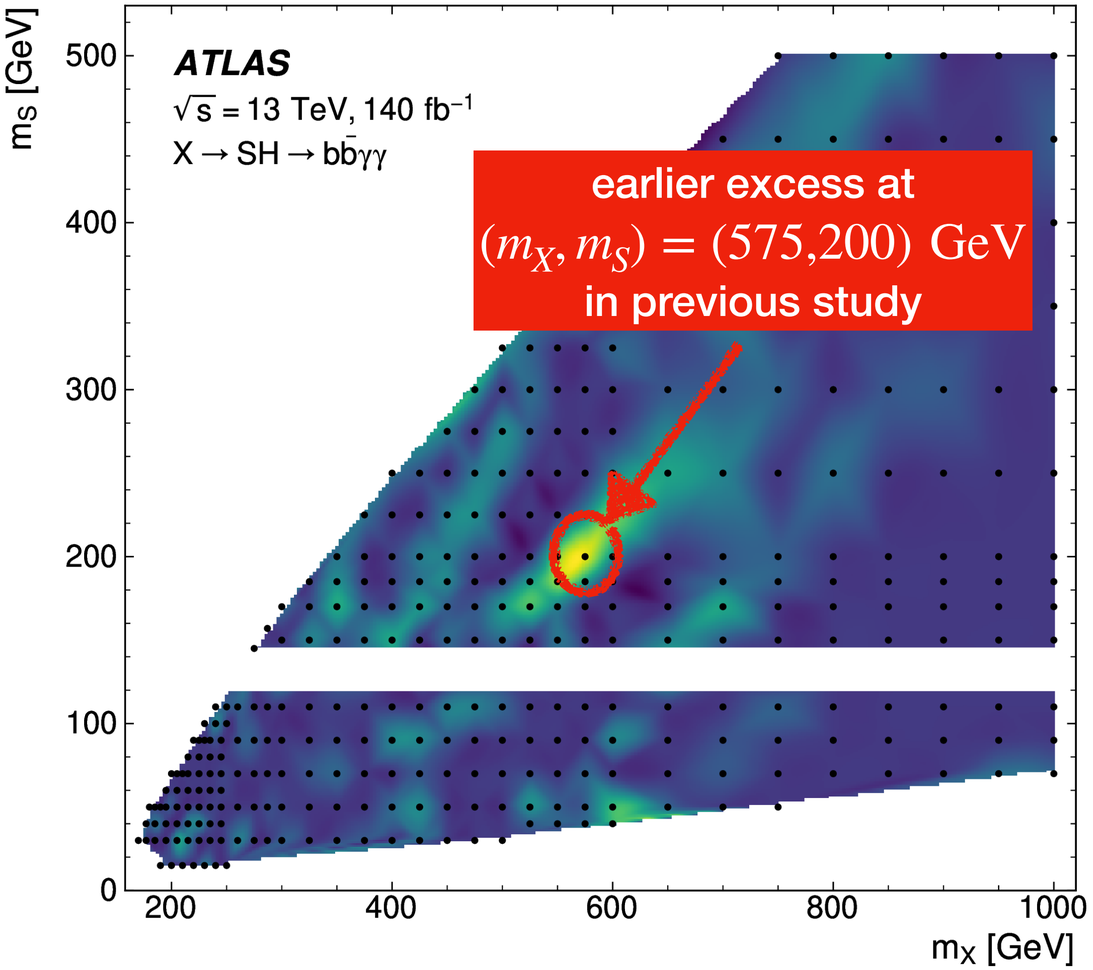

Our analysis using Run-2 + partial Run-3 data

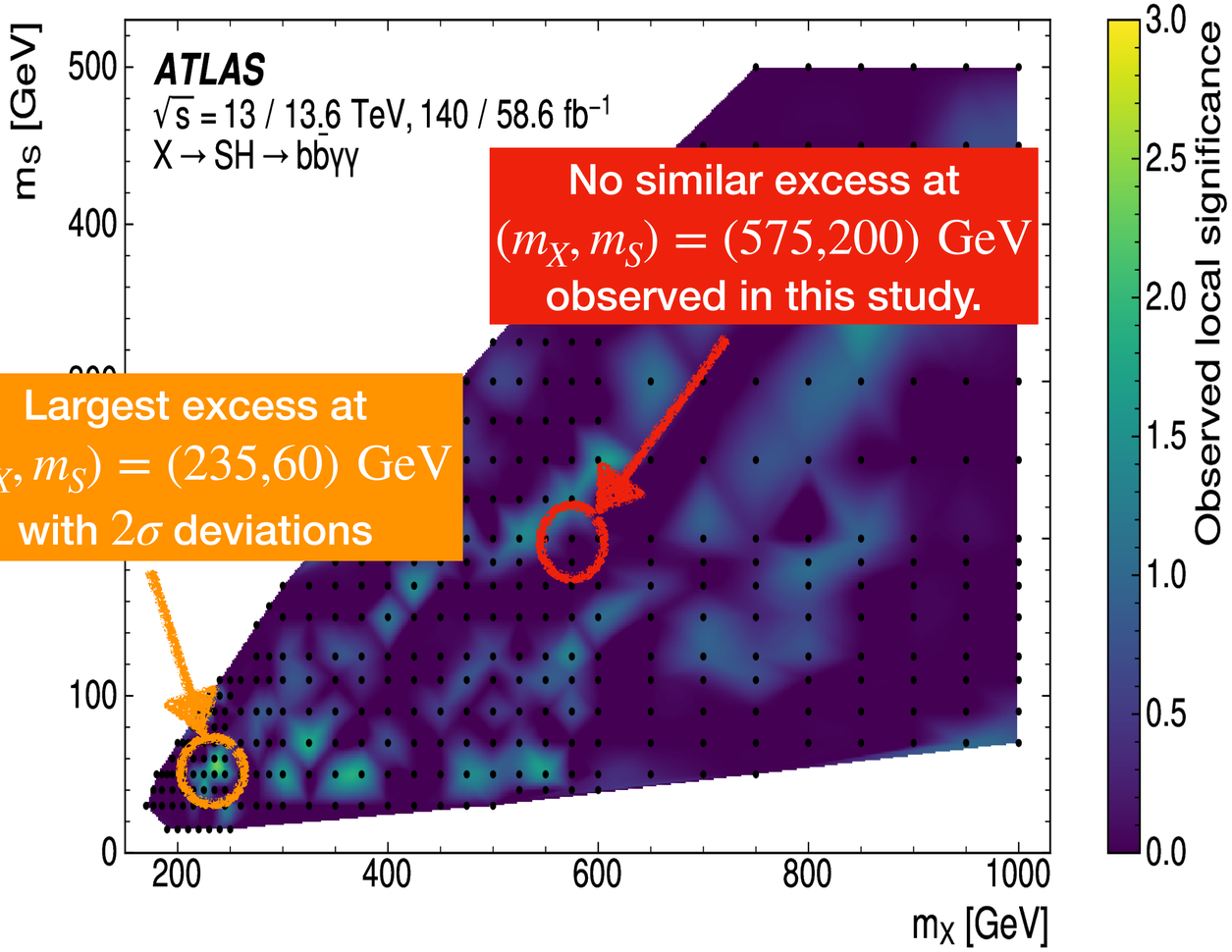

$(m_X, m_S) = (575,200)$ GeV

ATLAS Run-2 only analysis

[JHEP 11 (2024) 047)]

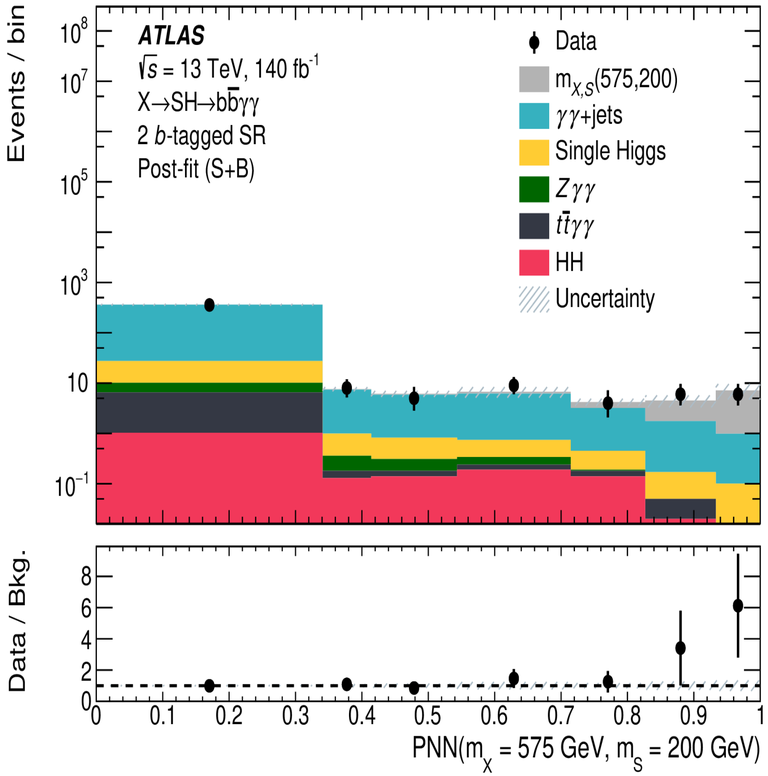

Our analysis using Run-2 + partial Run-3 data

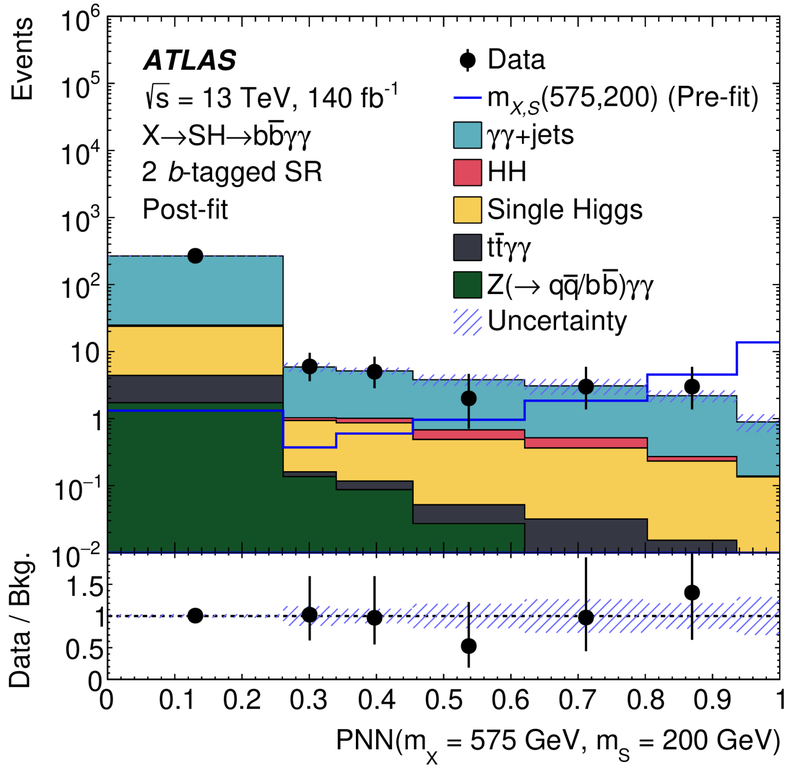

$(m_X, m_S) = (575,200)$ GeV

ATLAS Run-2 only analysis

[JHEP 11 (2024) 047)]

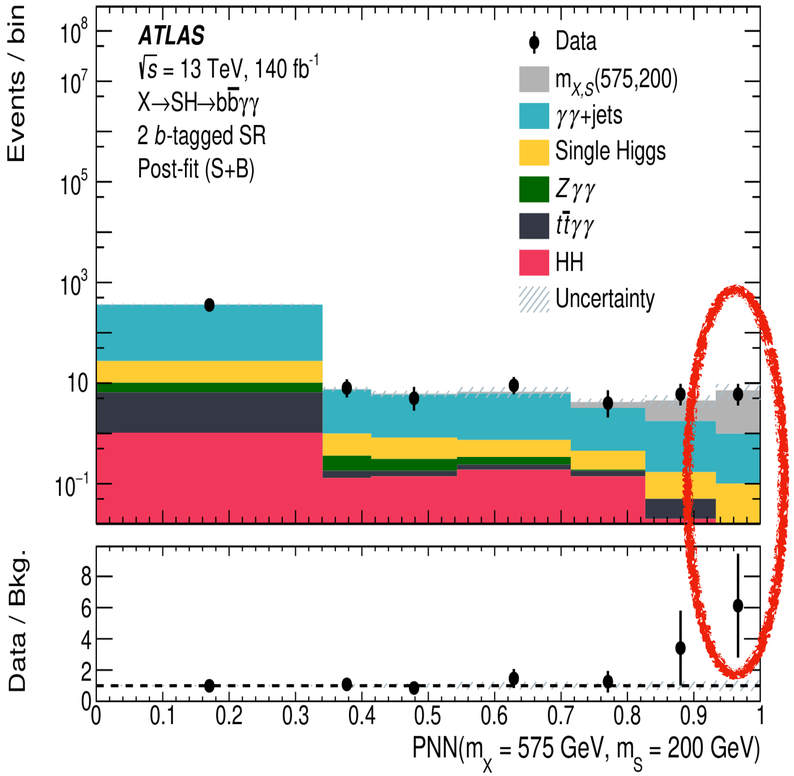

Our analysis using Run-2 + partial Run-3 data

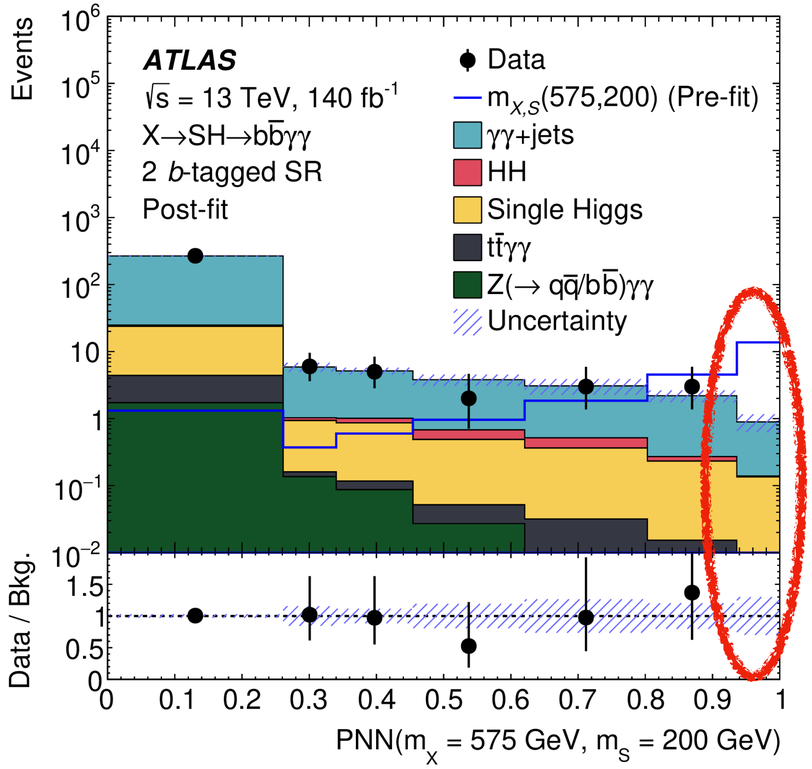

- *0 data events observed in the highest PNN score bin in our study while there were 6 in previous analysis*.

$(m_X, m_S) = (575,200)$ GeV

ATLAS Run-2 only analysis

[JHEP 11 (2024) 047)]

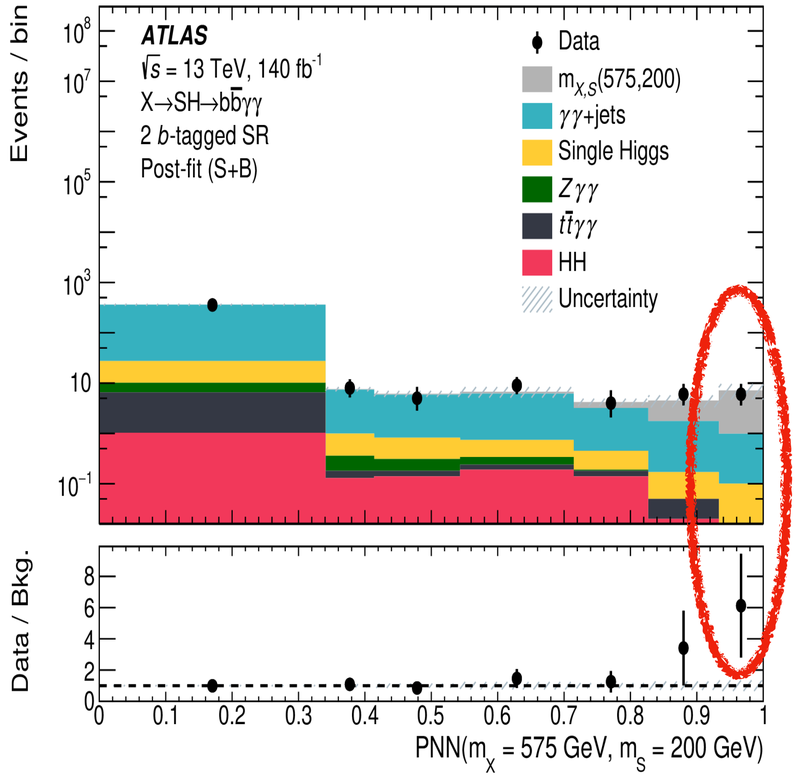

Our analysis using Run-2 + partial Run-3 data

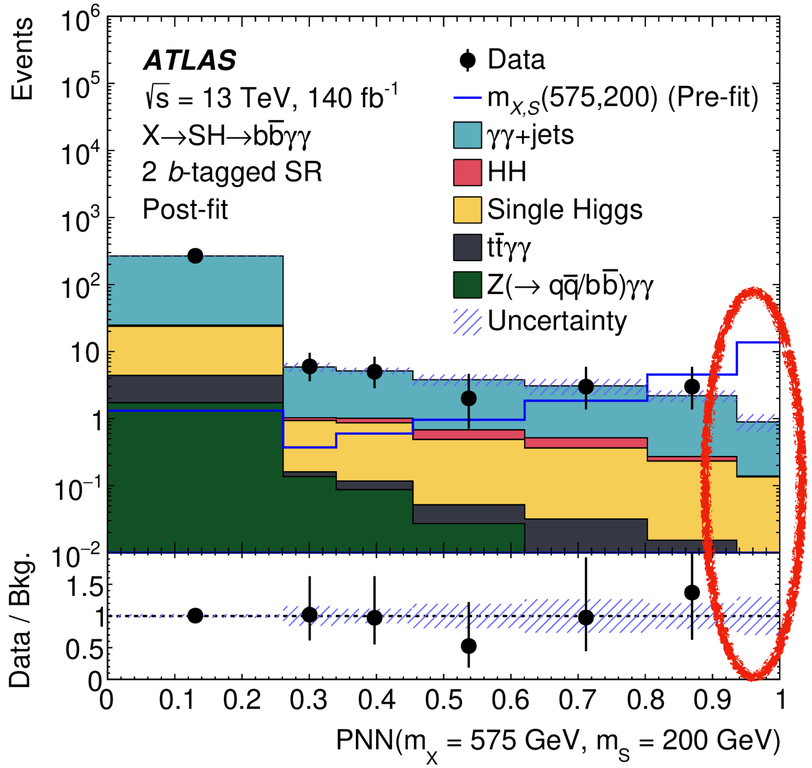

- *0 data events observed in the highest PNN score bin in our study while there were 6 in previous analysis*.

- ***Events contributing to earlier excess checked individually***:
  - Most of them ***fail 2 b-tagged preselection***.
  - smaller fraction ***fall outside the new narrower*** $m_{\gamma\gamma}$ ***mass window***.

Limits on $\sigma_{13\ \mathrm{TeV}}$

Limits obtained from our analysis using Run-2 + partial Run-3 data

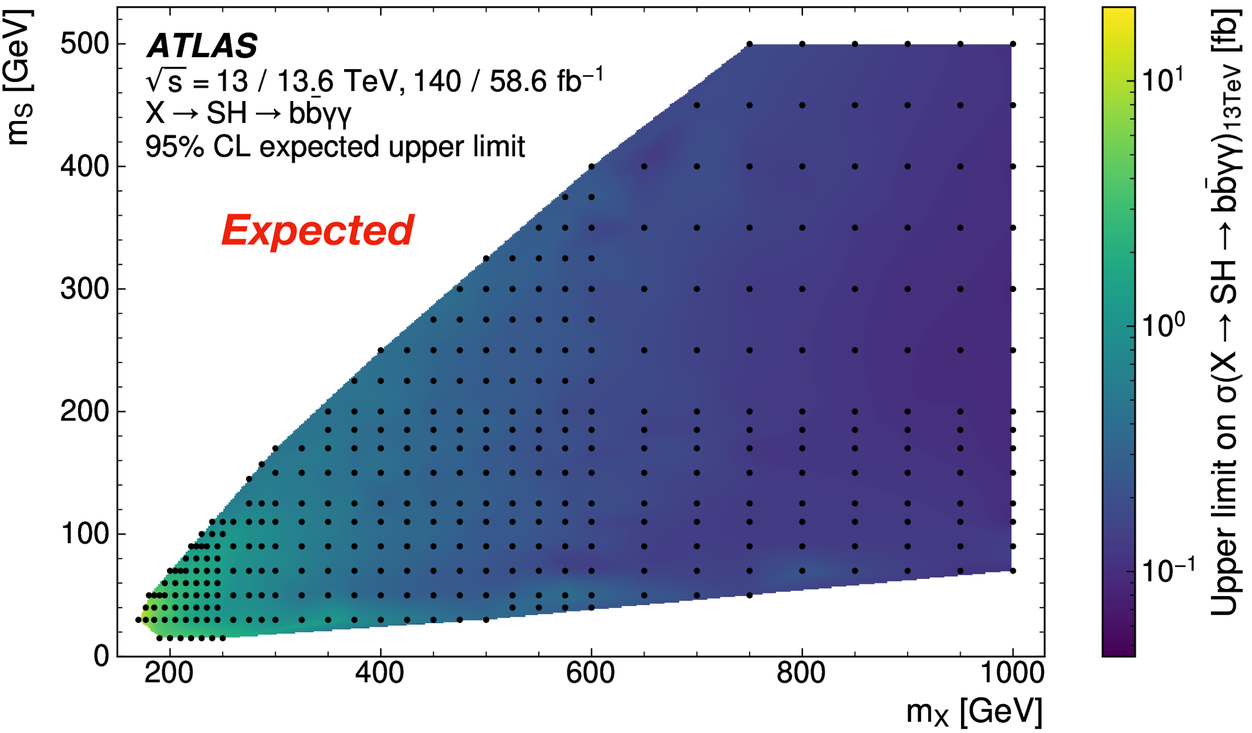

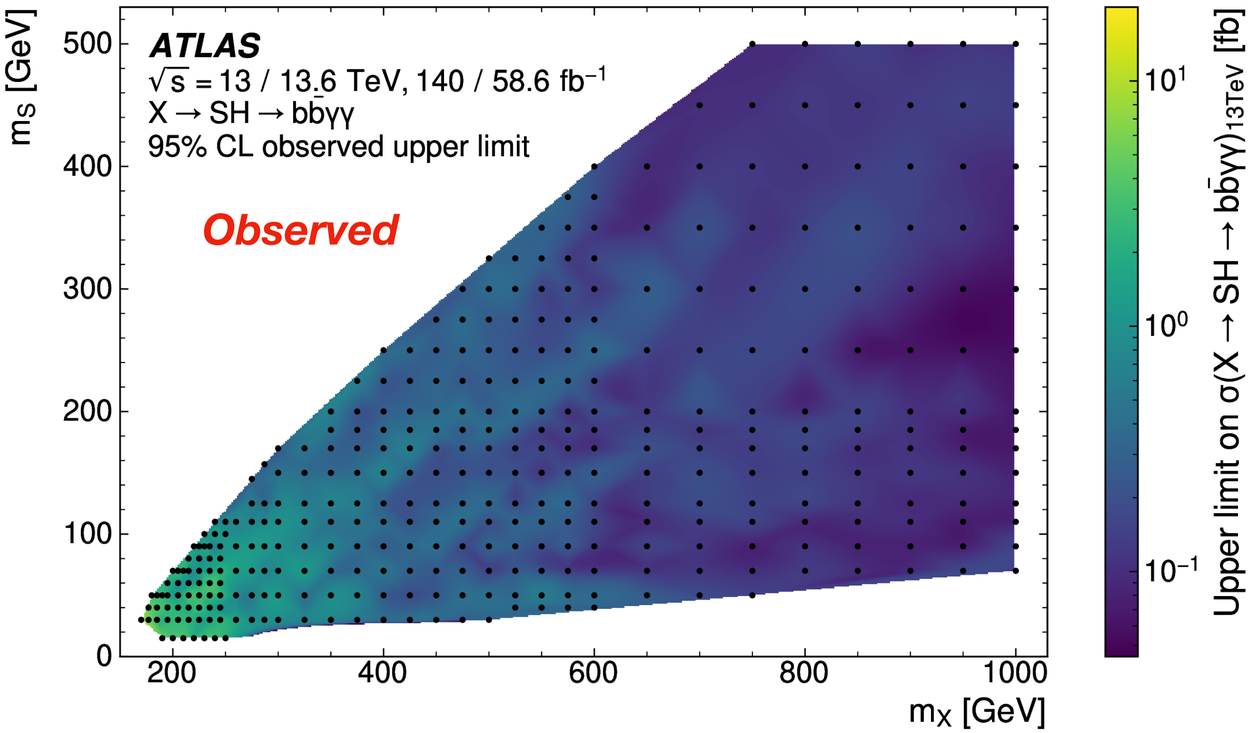

Generally better sensitivity in the high mass region, where signal kinematics differ more significantly from background.

Limits on $\sigma_{13\ \mathrm{TeV}}$

Ratio of expected limits from this study to Run-2 only analysis

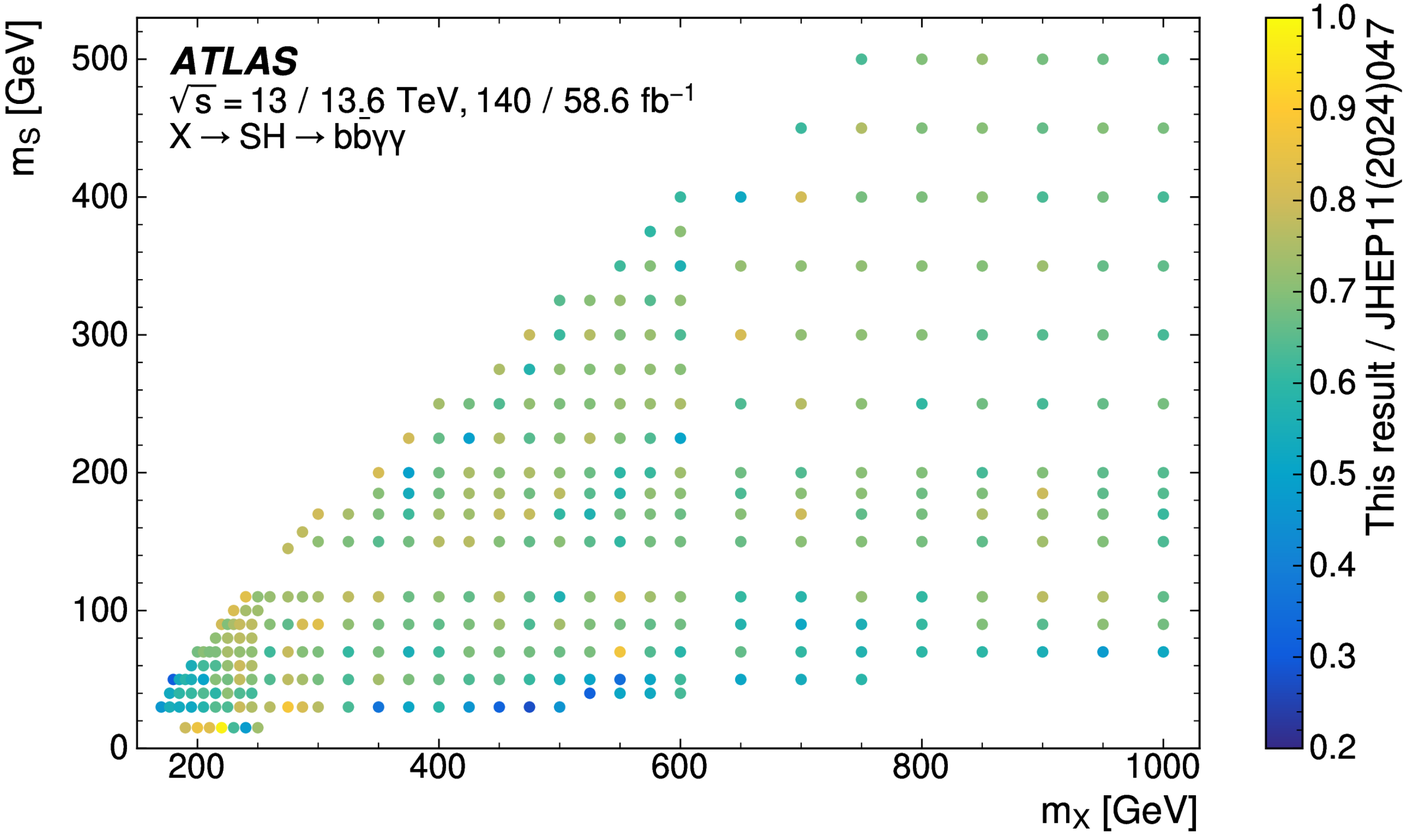

Distribution of ratios across all tested mass points

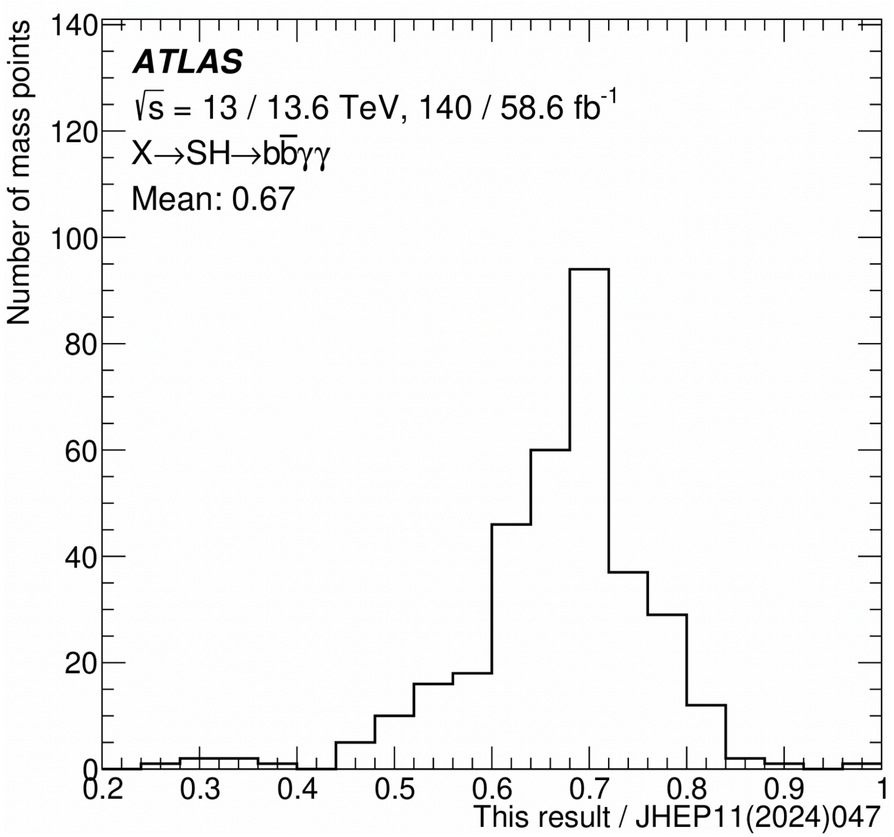

- *Expected limits 15 - 73 % better, with largest improvements in low-mass region, thanks to inclusion of Run-3 data and updates in SR definition, b-tagging, and in PNN training.*

Conclusion

- Updated search for $X \to S(\to b\bar{b})H(\to \gamma\gamma)$ following up on excesses from previous Run-2 analyses, *using Run-2 + partial Run-3 data*.
  - *Updated b-tagging with GN2 @ 85% signal efficiency WP.*
  - *Tighter SR $m_{\gamma\gamma}$ window.*
  - *4 separate PNN training with m_S included for 1 b-tagged.*

✓ Significant improvement in expected limits on $\sigma_{13\ \mathrm{TeV}}$.

✓ No similar excess @ $(m_X, m_S) = (575,200)\ \mathrm{GeV}$ observed and maximum local significance of 2σ @ $(m_X, m_S) = (235,60)\ \mathrm{GeV}$.

Backup

Table 1: Summary of the nominal signal and background samples. The generator used in the simulation, the PDF set, the showering model and the set of tuned parameters are also provided. When different from Run 2, settings used for the simulation of the Run-3 samples are indicated in parentheses.

Process	**Generator**	**PDF set**	**Showering**	**Tune**
$X \to SH$	Pythia 8.3 [30]	NNPDF2.3lo [31]	Pythia 8.3 [30]	A14 [32]
$\gamma\gamma$+jets	Sherpa 2.2.14 [34]	NNPDF3.0nnlo [45]	Sherpa 2.2.14	–
$t\bar{t}\gamma\gamma$	MadGraph5_aMC@NLO [44]	NNPDF2.3lo	Pythia 8.3	A14
$Z(\to q\bar{q}/b\bar{b})\gamma\gamma$	Sherpa 2.2.16	NNPDF3.0nnlo	Sherpa 2.2.16	–
ggF H	Nnlops [47–51]	PDF4LHC15 [52]	Pythia 8.3	AZNLO [46] (A14)
VBF H	Powheg Box v2 [53–56]	NNPDF3.0nlo [45] (PDF4LHC21 [52])	Pythia 8.3	AZNLO (A14)
WH	Powheg Box v2 [57, 58]	NNPDF3.0nlo (PDF4LHC21)	Pythia 8.3	AZNLO (A14)
$qq \to ZH$	Powheg Box v2	NNPDF3.0nlo (PDF4LHC21)	Pythia 8.3	AZNLO (A14)
$gg \to ZH$	Powheg Box v2	NNPDF3.0nlo (PDF4LHC21)	Pythia 8.3	AZNLO (A14)
$t\bar{t}H$	Powheg Box v2 [59]	NNPDF3.0nlo (PDF4LHC21)	Pythia 8.3	A14
$b\bar{b}H$	Powheg Box v2 [48]	NNPDF3.0nlo (PDF4LHC21)	Pythia 8.3	A14
tHq	MadGraph5_aMC@NLO	NNPDF3.0nlo	Pythia 8.3	A14
tHW	MadGraph5_aMC@NLO	NNPDF3.0nlo	Pythia 8.3	A14
ggF HH	Powheg Box v2 [56, 60, 61]	PDF4LHC21	Pythia 8.3	A14
VBF HH	MadGraph5_aMC@NLO	NNPDF3.0nlo	Pythia 8.3	A14

Table 2: SR and CR yields for the different processes before the likelihood fit described in Section 7. "Other Single Higgs" includes the following production modes: VBF H, WH, tHq, and tHW.

	Run 2				Run 3			
	1 b-tagged region		2 b-tagged region		1 b-tagged region		2 b-tagged region	
	SR	**CR**	**SR**	**CR**	**SR**	**CR**	**SR**	**CR**
$\gamma\gamma$+jets*	2652 ± 22	23740 ± 200	259 ± 4	2347 ± 19	1119 ± 22	10060 ± 200	106.3 ± 2.9	967 ± 19
$t\bar{t}\gamma\gamma$	3.84 ± 0.20	34.2 ± 1.8	2.78 ± 0.18	25.2 ± 1.6	1.80 ± 0.12	16.0 ± 1.1	1.33 ± 0.13	11.8 ± 1.2
$Z(\to q\bar{q}/b\bar{b})\gamma\gamma$	4.86 ± 0.28	42.5 ± 2.6	2.01 ± 0.17	18.1 ± 1.5	2.24 ± 0.20	20.6 ± 1.6	0.81 ± 0.11	8.1 ± 0.9
ggFH+$b\bar{b}H$	70 ± 70	16 ± 15	8 ± 7	1.6 ± 1.5	37 ± 33	10 ± 10	3.5 ± 3.3	0.9 ± 0.9
$t\bar{t}H$	8.6 ± 1.1	1.53 ± 0.29	8.0 ± 1.0	1.39 ± 0.27	3.9 ± 0.5	0.86 ± 0.33	3.6 ± 0.5	0.76 ± 0.30
ZH	6.5 ± 0.6	1.20 ± 0.24	3.54 ± 0.32	0.60 ± 0.12	2.85 ± 0.32	0.65 ± 0.23	1.48 ± 0.20	0.31 ± 0.12
Other Single Higgs	20 ± 13	3.8 ± 2.6	2.0 ± 0.8	0.35 ± 0.16	9 ± 6	2.2 ± 1.6	0.9 ± 0.4	0.20 ± 0.11
HH	1.26 ± 0.08	0.24 ± 0.04	1.49 ± 0.12	0.28 ± 0.05	0.56 ± 0.06	0.15 ± 0.04	0.68 ± 0.09	0.17 ± 0.05
Total	2770 ± 70	23840 ± 200	286 ± 8	2395 ± 20	1180 ± 40	10110 ± 200	119 ± 5	989 ± 20
Data	2669	23838	287	2395	1179	10114	127	989

* The normalisation factors for the $\gamma\gamma$+jets background are applied, but their uncertainties are not included in the $\gamma\gamma$+jets uncertainties.

PNN Input features for 1 *b*-tagged

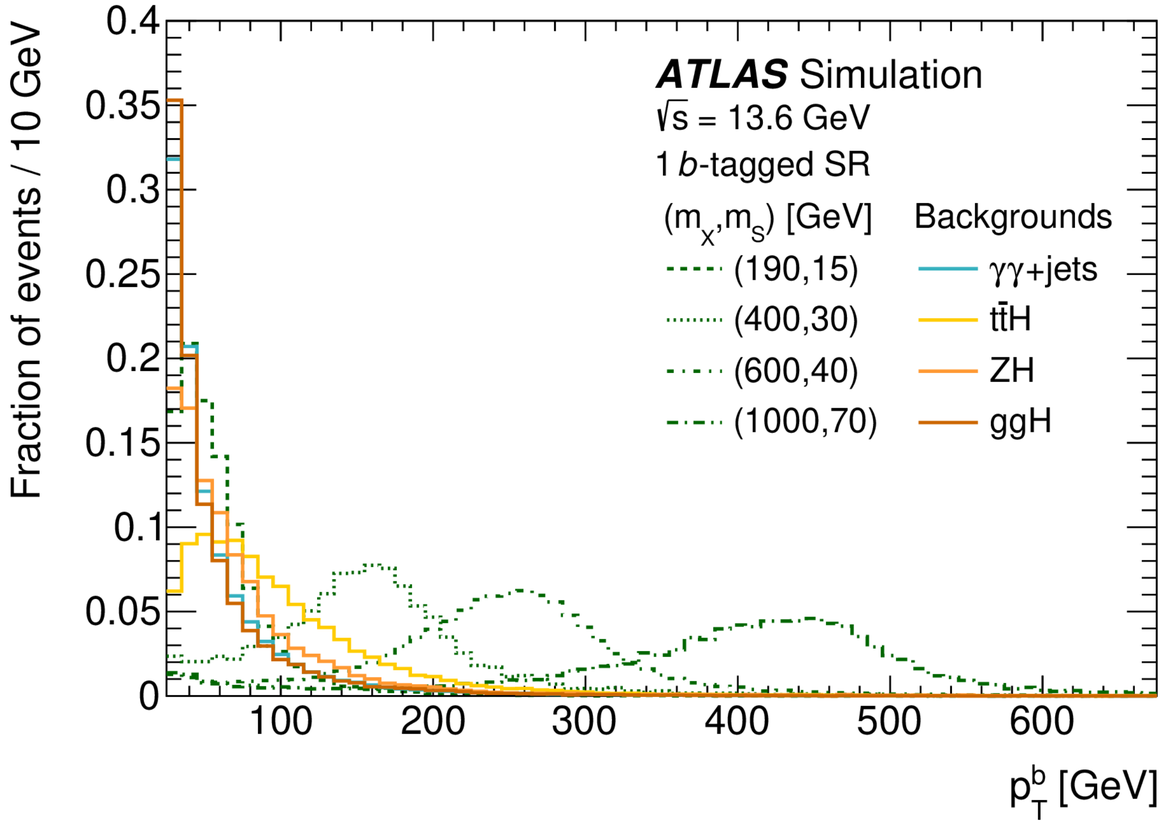

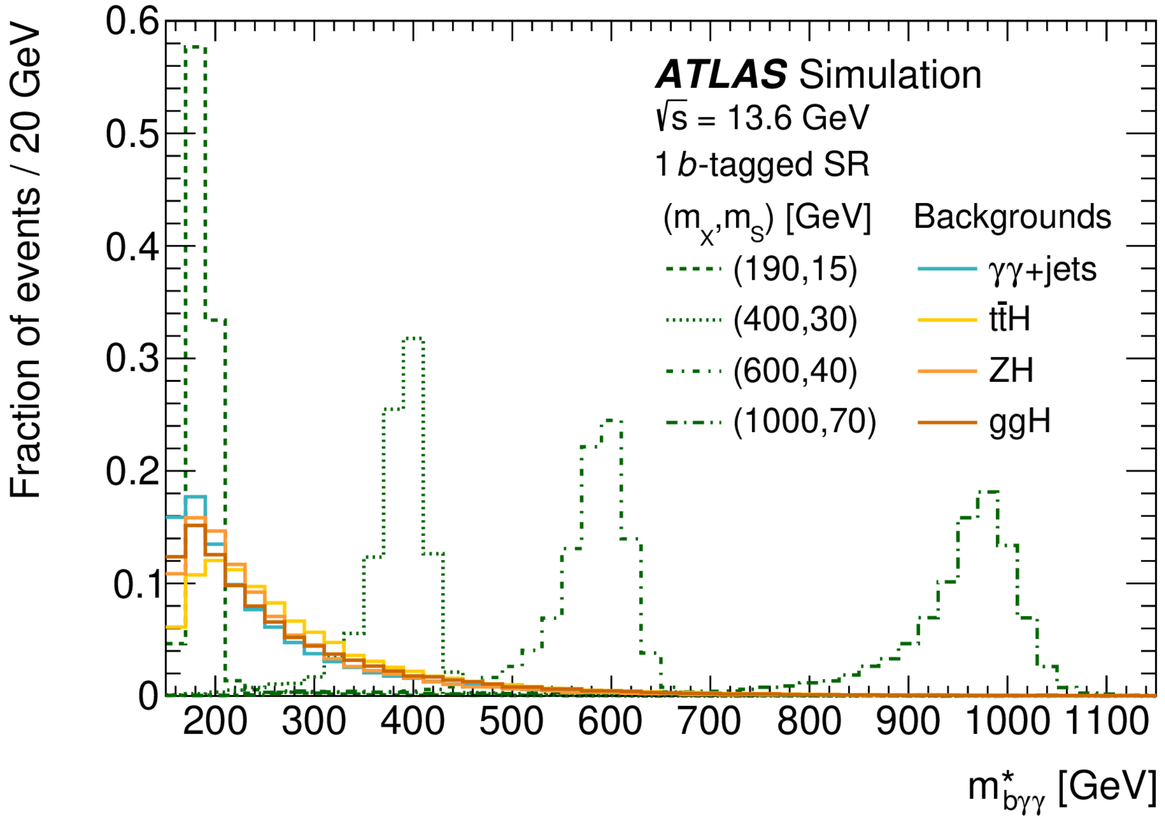

Post-fit PNN @ (1000, 70)

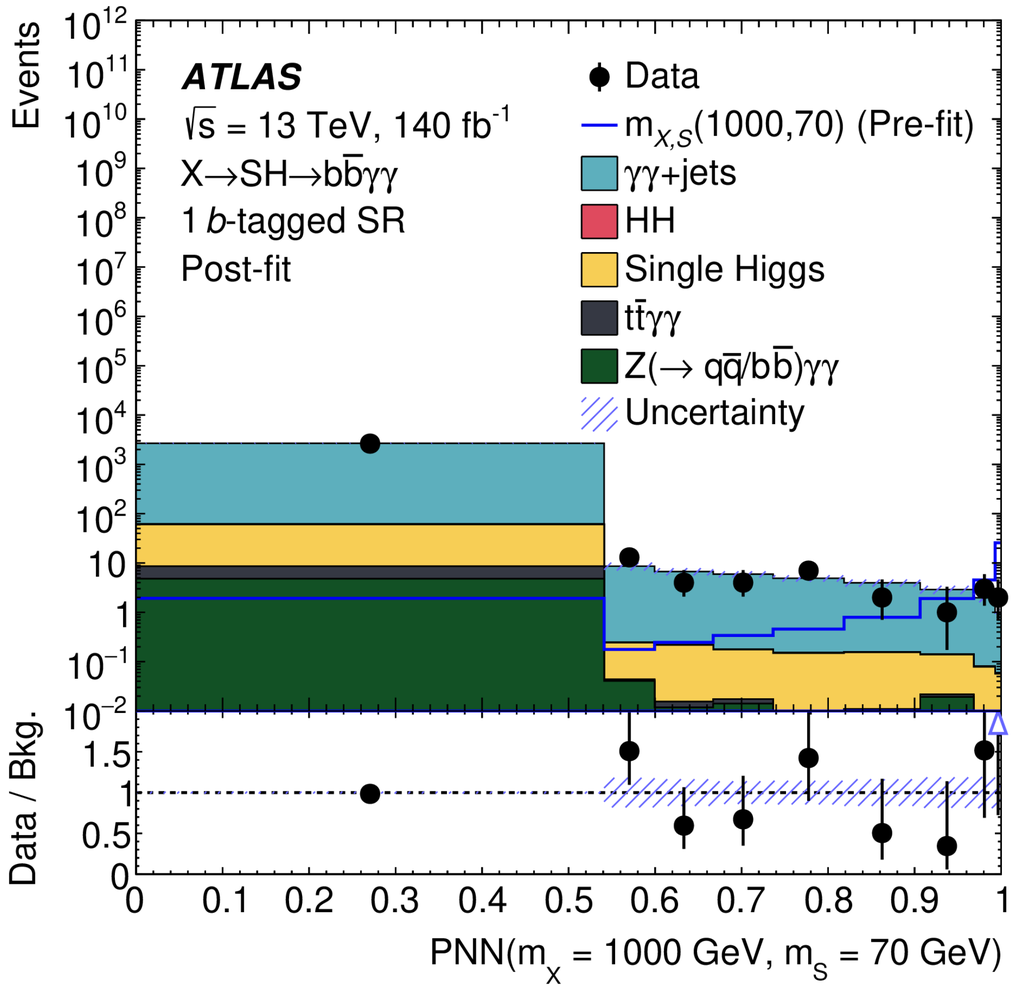

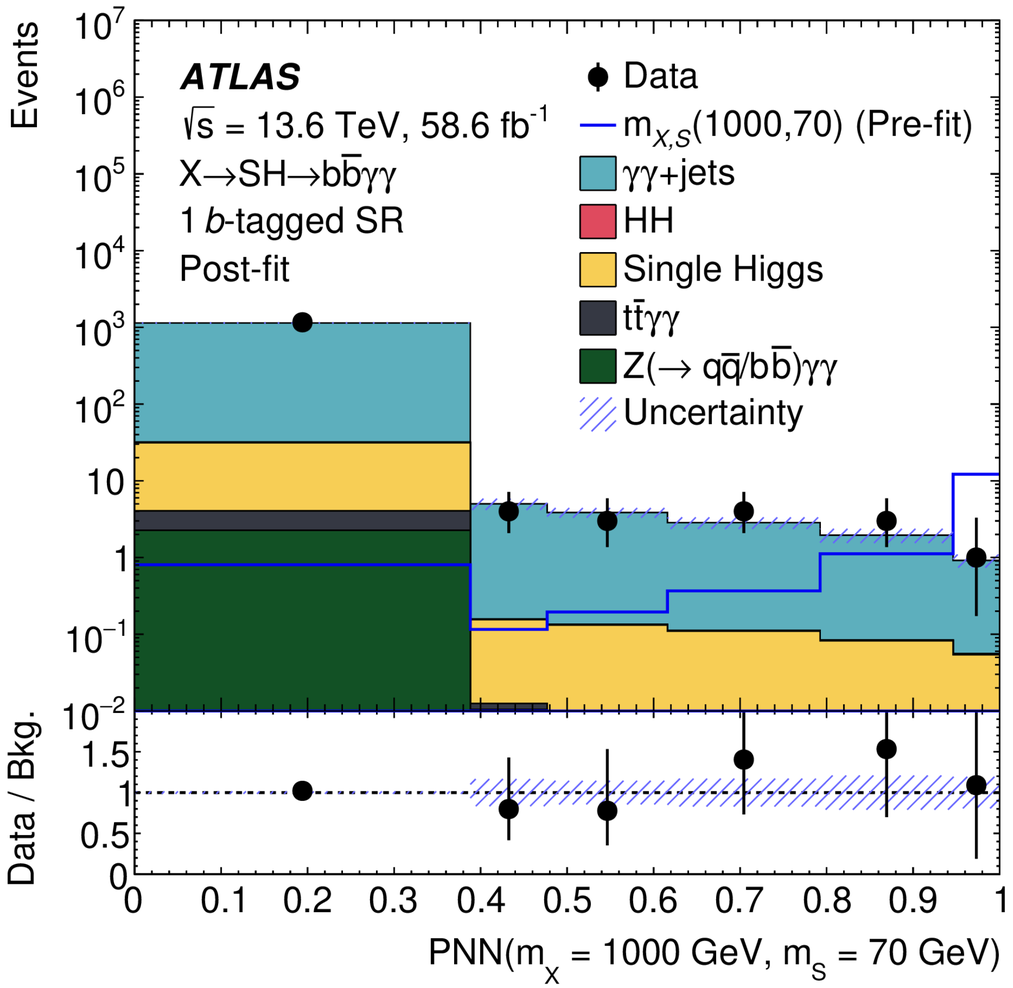

PNN before and after linear correction

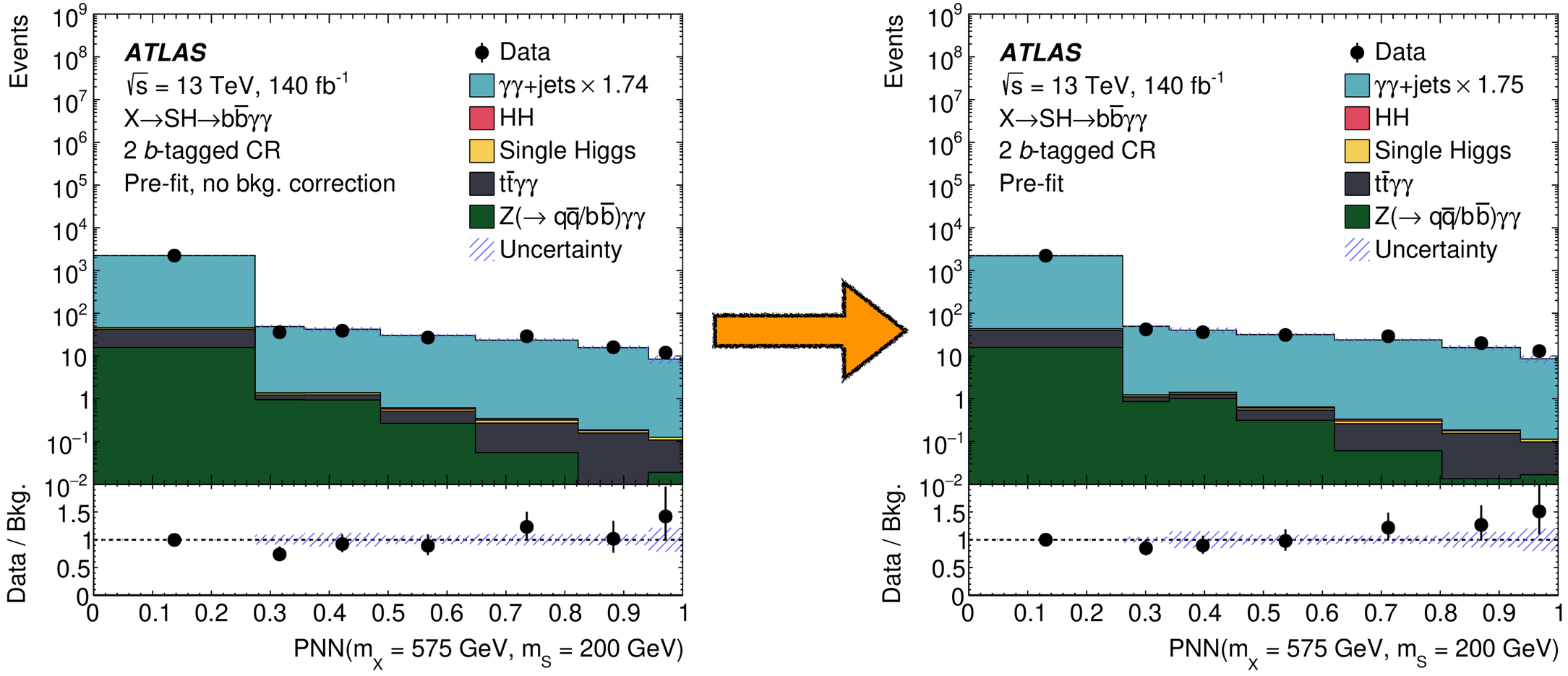

$\sigma_{13.6\ \mathrm{TeV}}/\sigma_{13\ \mathrm{TeV}}$ by Pythia 8.3

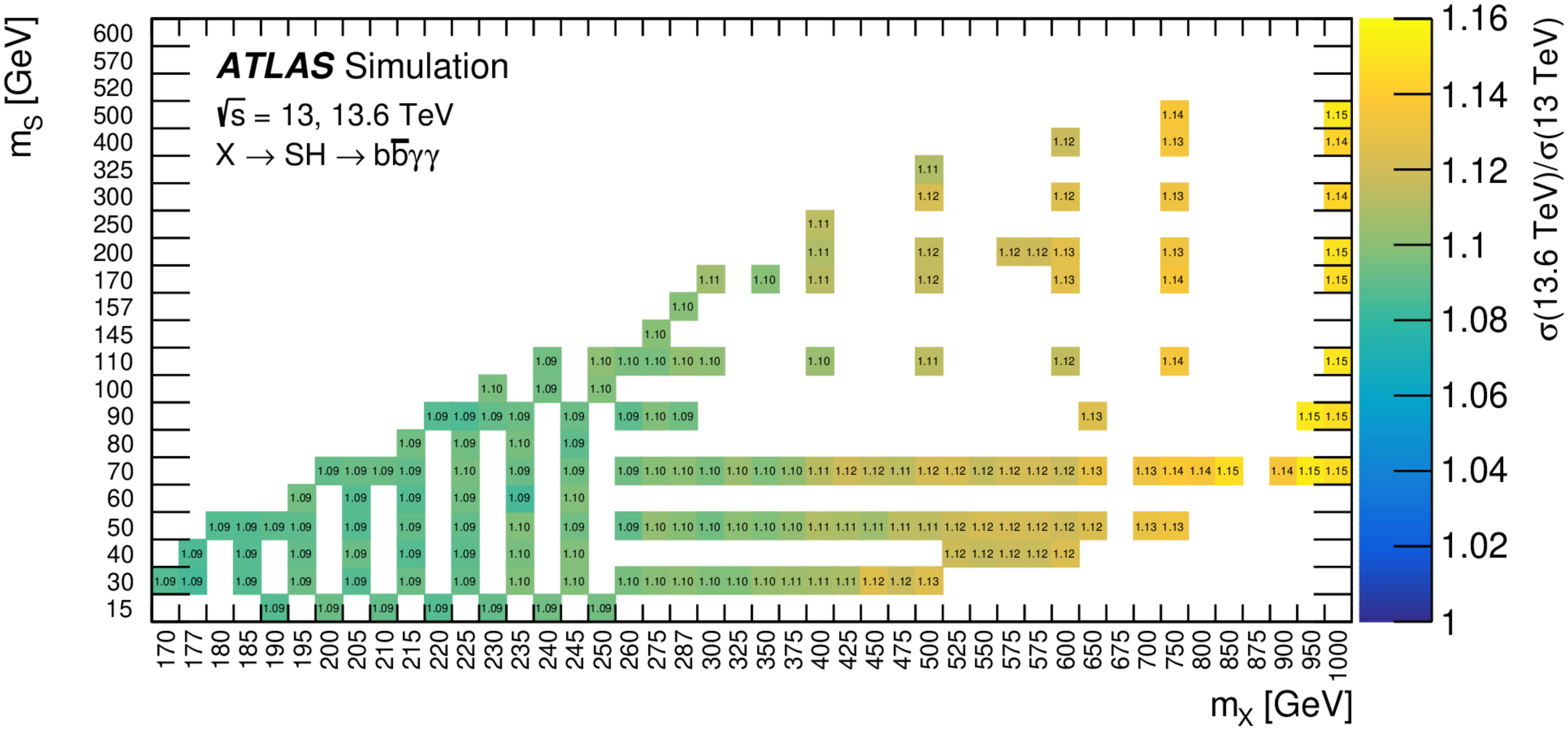

Limits on $\sigma_{13.6\ \mathrm{TeV}}$